A review of evidence for a Gulf of Tonkin location for the Australasian tektite source crater

Aubrey Whymark [1]*

[1]Consultant Wellsite Geologist, Manila, Philippines.
* Corresponding author: aubrey@tektites.info
Received 5 March 2021 ; Accepted 17 June 2021.

Abstract

Australasian tektites (AAT) occur across Southeast Asia, Australia, the Indian Ocean, and southwest Pacific Ocean. AAT form the youngest and most extensive major tektite strewn field. Unlike other tektite strewn fields, AAT have no known source crater. Review of the literature establishes that a single ~43 km post-impact diameter crater exists, possibly significantly enlarged by slumping. The obliquity of the impact that formed the AAT would result in a crater that is less pervasive in depth but with greater downrange shock effects and melt ejection. Multiple lines of evidence, historically viewed in isolation, were examined, concatenated, contextualized, and discussed. Tektite morphology and distribution; microtektite regressions; geochemical considerations, comparisons, and iso-concentration regressions; lithological characteristics; age of source rock; and regional geological considerations are reviewed. The source material is predicted to be an abnormally thick sequence of rapidly deposited, poorly compacted, deltaic to shallow marine, shales to clay-rich siltstones of early Pleistocene to Pliocene age. The impact likely occurred in a shallow marine environment. Forty-two maps of positive and negative parameters are presented and overlain. These indicate the AAT source crater probably lies in the central to northwestern Yinggehai - Song Hong Basin / Gulf of Tonkin. This geochemically optimal setting is characterized by exceptionally high sedimentation rates that explain the ^{10}Be and Rb-Sr age discrepancy, the seawater signature, and apparent absence of a crater by rapid burial.

1. Introduction

Tektites are naturally occurring, holohyaline, macroscopically homogenous, droplets formed by the melting and ballistic ejection of silica-rich target rocks by large cosmic impacts. Australasian tektites (AAT) form a young and extensive strewn field covering over 10% of the Earth's surface. All major tektite groups, apart from the AAT, have been geochemically associated with terrestrial impact craters. AAT have been extensively studied, drawing data from diverse and disparate fields, each yielding conclusion in isolation. This article attempts to concatenate all available evidence to identify the probable AAT source crater location.

2. Constraints

2.1 Presence of a Crater: All other known tektite strewn fields are associated with craters. The existence of silica-rich ballistic ejecta with low-angle trajectories and velocities exceeding 5 km/s (Chapman, 1964) demonstrates a direct transfer of energy, as opposed to an aerial burst (Wasson, 2003), or impact plume (Wasson, 2017) scenario. An impact crater is concluded to exist.

2.2 Single or Multiple Craters: The distance of ejection can be related to crater size, which in turn is a function of the mass and velocity of the impactor (Elliott, Huang, Minton, & Freed, 2018). Other factors, such as obliquity of impact and target composition, also influence

distance of ejection and are discussed in Section 2.6. The distance between the most northerly Indochinese macro-tektites and most southerly Australian macro-tektites exceeds 8,500 km. The implication is that at least one large impact crater is present. A thorough review of the geochemistry of tektites (Schnetzler & Pinson Jr, 1963), concluded that a random process of formation or multiple separate impacts could be excluded. Nd and Sr isotopic variations indicate a single impact event (Blum, Papanastassiou, Koeberl, & Wasserburg, 1992; Shaw & Wasserburg, 1982). Rare-earth elements (REE) indicate a single reasonably uniform source (Koeberl, 1994; Koeberl, Kluger, & Kiesl, 1985). It is concluded that a single large crater in a relatively homogenous source rock exists. Associated smaller craters in the same source rock cannot be excluded but are not required.

2.3 Age: AAT are 786 ± 2 ka based on ^{40}Ar/^{39}Ar dating of tuffs at ODP Site 758 and relative stratigraphic position to Termination IX (Mark et al., 2017) or 788.1 ± 3 ka based on the ^{40}Ar/^{39}Ar age data from four AAT (Jourdan, Nomade, Wingate, Eroglu, & Deino, 2019). The impact occurred during a glaciation where the continental shelf would be subaerially exposed or covered by very shallow seas. The young age means that geological evidence of the structure could not have been eroded away. The structure exists, even if buried. The recent age of ejecta means that the tektite distribution suffers little stratigraphic outcrop bias. Plate tectonic shift of the crater and ejecta has a low significance over this short period of time, but in high resolutions should be considered.

2.4 The Crater Size: Utilizing microtektite data and the methodology of Stöffler, Gault, Wedekind, & Polkowski (1975), which is calibrated to known impacts and thus has a high expectation for accuracy, a post-impact crater diameter of 32 ±14 km is derived (Glass & Pizzuto, 1994), or 33 ± 8 km (Prasad, Mahale, & Kodagali, 2007). If un-melted ejecta estimates are considered, which should provide an even more accurate estimate, a 39 to 44 km (Glass, 2003) and 43 ± 9 km (Glass & Koeberl, 2006) diameter crater estimate is

derived. Studying the compositional range of condensate droplets (bottle-green microtektites), which reflect plume cooling rate and therefore plume size, a 40 to 60 km diameter crater was estimated (Elkins-Tanton, Kelly, Bico, & Bush, 2002).

Tektite distribution can be compared with tektite / spherule strewn fields that have a known crater, but source rock, fluid content, sea depth, and impactor parameters, particularly velocity and obliquity of impact may have varied. It can be crudely ascertained that the AAT source crater is likely larger than the 24 km diameter (Schmieder & Kring, 2020) Ries Crater, significantly smaller than the 100 km diameter (Schmieder & Kring, 2020) Popigai Crater, and broadly comparable with the 40 to 45 km (Schmieder & Kring, 2020) Chesapeake Bay Crater, with slumped outer rim of 80 to 90 km (Collins & Wünnemann, 2005).

In conclusion, a crater with 43 ± 9 km diameter (Glass & Koeberl, 2006) should be sought. If the crater is in a continental shelf setting then, post-impact, it may be slumped to 80 to 90 km or more in diameter.

2.5 Obliquity of Impact / Crater Geometry: The AAT impact was oblique, and this is very adequately demonstrated by asymmetric morphological and geochemical variations of tektites that indicate the source crater is in the broad Indochinese portion of the strewn field. The obliquity of the impact would reduce the depth and volume of melted and shocked materials at the impact site and enhance the volume of ejected melt (including tektites) (Pierazzo & Melosh, 2000). However, highly oblique impacts (<5°) may have a negative effect on tektite production as the first formed ejecta must travel a greater distance to traverse the atmosphere.

To establish whether the impact was a highly oblique (<5°) grazing impact, or an oblique (5° to 30°) impact the distal ejecta pattern should be reviewed. The AAT strewn field has a downrange lobe of ejecta, mirroring forbidden zones, and butterfly lobes, typical of impacts below 45° (Gault & Wedekind, 1978). The bilateral symmetry of the downrange ejecta is broadly along a 164° azimuth and the butterfly lobes are ~62° offset from the center

of the downrange ejecta. In grazing impacts that produce elliptical craters a 90° offset from the center of the downrange ejecta would be anticipated (Gault & Wedekind, 1978).

Highly oblique grazing impacts result in increased projectile contamination of the target melt (Artemieva & Pierazzo, 2003; Stöffler, Artemieva, & Pierazzo, 2002), something not observed in AAT.

In a grazing impact there should be an uprange forbidden zone, but in less oblique impacts the uprange forbidden zone may close as the impact proceeds (Schultz, Anderson, & Hermalyn, 2009; Schultz et al., 2007). Therefore, the presence of uprange tektites is an argument against a grazing impact. This will be discussed further as the evidence is presented.

AAT distribution suggests an oblique impact above 5° but, by comparison to Artemieva (2013), under 30°. An oblique impact is optimal for melt (tektite) ejection (Pierazzo & Melosh, 2000) and will limit downward shock effects at the impact site. The impact crater might be asymmetrical in its depth profile, deeper in a north-northwesterly direction, after Gault & Wedekind (1978). If there was subsequent slumping this may be influenced by the asymmetry of the post-impact crater profile and might result in an elliptical slumped crater. The above factors may result in a less pervasive crater with atypical morphology. This would make recognition more problematic.

2.6 Tektite Morphological Regression: AAT fall into three transitional but readily differentiable morphological groups, which can be compared with tektites in strewn fields with a known source crater. Distal tektites (e.g., Australites) were the first formed, highest velocity tektites. They underwent minimal plastic deformation as the molten body exited the atmosphere, suffered ablation during re-entry, then spallation. Medial tektites (e.g., Philippinites, Billitonites, and Bediasites) underwent moderate plastic deformation as the molten body exited the atmosphere, re-entry heating that was insufficient for ablation to occur, and then spallation. Proximal tektites (e.g., Indochinites, Moldavites, Georgiaites, Ivory Coast Tektites) underwent significant

plastic deformation as they interacted with the atmosphere at lower altitudes, suffered minimal re-entry heating and minimal spallation. Muong Nong-type (MN-type) layered impact glass, whilst ballistically ejected, never formed discrete surface tension-controlled droplets due to lower melt temperature. MN-type layered impact glasses represent the lowest energy, theoretically most proximal, melts.
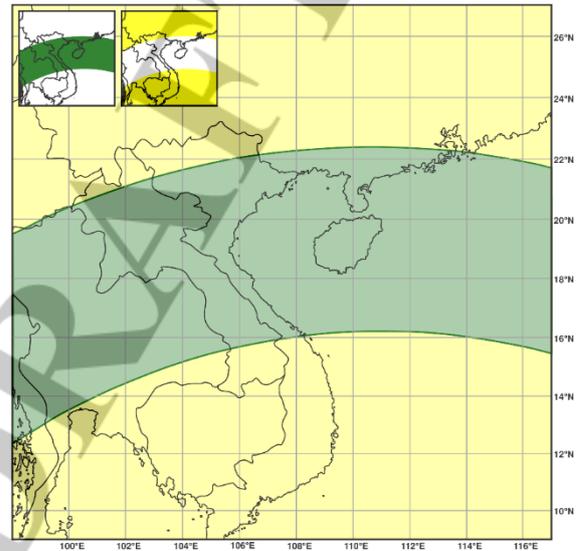
Fig. 1: Taking Sangiran, Java, as the 5 km/s mark, where the most northerly directly downrange ablated tektites exist, the crater likely lies somewhere between 3,319 km away (37° ejection angle) and 2,632 km away at 20° and 56.8° ejection angle. The AAT crater probably lies within the belt highlighted in green. The middle to southerly portion of the green shaded region is most probable based on a 20° to 25° re-entry angle for tektites in Java. The yellow area is lower probability. Inset: Data used in map overlay. Green = Probable regions; Yellow = Less favorable regions for the AAT impact.

The lower ablation limit for tektites is about 5 km/s (Chapman, 1964). This is the defining boundary between medial and distal tektite morphologies. Within the AAT strewn field, the most northerly ablated downrange tektites are found in Sangiran, Java (Chapman, 1964). To the north (along an azimuth towards Indochina), tektites are not ablated and therefore re-entered at velocities below about 5 km/s. Taking Sangiran, Java, as the 5 km/s mark, and utilizing trajectory calculations from *Orbit 1.2 Software* (1998-2000), the crater likely lies somewhere between 3,319 km away (37° ejection angle) and 2,632 km away at 20°

and 56.8° ejection angle (shown in **Fig. 1**). At ejection angles lower than 20° or higher than 56.8° (which are less likely) the crater will be even closer. A potential margin of error of hundreds (but not thousands) of kilometers exists, but this calculation indicates the most probable impact region and rules out the wildest crater guesses where modelled re-entry velocities do not match observed physical attributes of the tektites. Re-entry angles of tektites over Java were likely quite oblique with angles of 20° to 25° probably being realistic, implying a distance from the source crater of 2,632 km to 2,992 km, again within a margin of error being present.

Increased target rock compressibility can enhance melt production (Stöffler, Hamann, & Metzler, 2018). Obliquity of impact can enhance melt ejection (Pierazzo & Melosh, 2000). Water-rich surface layers can potentially enhance melt production and ejection (K. T. Howard, 2011). These factors, together with the size of the impact, result in greater tektite abundance (assuming suitable source rocks) and distance of ejection (asymmetrically in the case of oblique impact). Regardless of scaling, the distal, medial, and proximal tektite morphological divisions would be expected to be found at broadly the same distance from the impact location. This is because the morphological divisions are primarily related to reentry heating, controlled principally by velocity. A tektite must travel from the crater location to a fall location. It can theoretically do so by any combination of angle and velocity that achieves the defined distance. Ejection angles of 15° to 50° result in tektite velocities of: 2.87 to 3.74 km/s to land at 900 km; 3.70 to 4.50 km/s to land at 1,650 km; and 6.40 to 7.05 km/s to land at 6,800 km from the impact location (*Orbit 1.2 Software*, 1998-2000). Velocity values are reasonably constrained regardless of the ejection angle.

Oblique impacts result in a low-angle downrange ejection of the highest velocity melts compared to vertical impacts that result in higher angle omnidirectional ejection of melt (Gault & Wedekind, 1978). The melt will travel further in oblique impacts, but at lower angles. In more energetic oblique impacts, sufficient energy is present in the later stage of impact to yield high-angle omnidirectional melts as well as the initial higher velocity low-angle downrange melt ejecta. So, at a set distance from the impact crater the ejecta may be low-angle melts derived from a smaller oblique crater or (low and) high-angle melts derived from a larger oblique or vertical impact. Morphological differences would be anticipated between low- and high-angle melt ejecta. Low-angle tektites will encounter greater atmospheric interaction. This manifests morphologically in cascading to smaller bodies in a hot melt, or by plastic deformation in a cooler more viscous melt during exit, and in a longer duration of heating during re-entry.

The question arises whether magnitude and obliquity of impact, which may affect ejection angle, influences the distance at which morphological groups theoretically occur. In short, it does, but to a minimal degree: this methodology will not offer precision but is expected to deliver a broadly accurate result. This is because re-entry velocity does not vary dramatically in response to expected re-entry angles at a fixed location. It is the tektite velocity that defines the boundary between distal and medial forms. The medial to proximal boundary is a little more complex: again, the medial morphology requires a certain re-entry velocity / heating, but spallation can be over-ridden by the glass temperature in the re-entry phase. If the glass retained sufficient temperature from formation, crack growth and spallation is inhibited. Scaling may have greater influence in the proximal realm, but the prerequisite for sufficient velocity to produce medial cores validates that all medial cores should be found at similar distances from the source. Variations in core morphology are illustrated in Fig. 11 of Chapman, (1964). Uncertainty in comparisons may be reduced further by comparing tektites from similar craters in terms of magnitude, obliquity, and target.

The distance of proximal and medial North American tektites from the Chesapeake Bay source crater can be compared with Australasian tektites. The two impacts are comparable in terms of calculated magnitude and can be inferred to have similar target rock characteristics as both impacts yield

widespread tektites. The asymmetry of the North American tektite distribution suggests the Chesapeake Bay impact was oblique, although likely less oblique than the AAT impact. Within the North American strewn field, the medial tektite morphologies are found at distances of 1,955 km to 2,180 km (O'Keefe, 1963) southwest from the point of impact. The proximal North American tektites are found predominantly to the southwest at distances of 635 km to 930 km (Povenmire, 2010; Povenmire & Strange, 2006). The comparable Chesapeake Bay impact is used to evaluate the AAT impact crater location.

The Central European strewn field yields proximal tektites at distances of 185 km to 430 km (Čada, Houzar, Hrazdil, & Skála, 2002; Trnka & Houzar, 2002) from the Ries source crater. The Ivory Coast strewn field yields tektites at distances of 255 to 320 km (Gentner, 1966) from the Bosumtwi source crater. These smaller impacts demonstrate that true tektites can occur in closer proximity to the crater.

The North American Bediasites are morphological equivalents to Philippinites, Malaysianites, Brunei tektites, Billitonites and northern Indonesianites. In North America similar morphologies occur at distances of 1,955 to 2,180 km (O'Keefe, 1963) from the impact site and do not occur within 930 km (Povenmire, 2010) from the impact site. All locations within 930 km of medial tektite occurrences can be eliminated as shown in red in **Fig. 2**. It can be established that by 1,955 km there are no proximal tektite morphologies (the true number is likely much less but cannot be calibrated). The source crater must be within 1,955 km of all proximal tektite morphologies. This further restricts the potential source area (green region in **Fig. 2**). A focal point can be established by assuming all proximal tektites occur within 930 km of the impact site. The actual number is somewhere between 930 and 1,955 km but likely close to the lower limit for the AAT when cross referenced with other evidence presented in this article. The focal point is therefore an area of highest probability but does not rule out surrounding areas. This approach is demonstrated by the dark green region in **Fig. 2**.
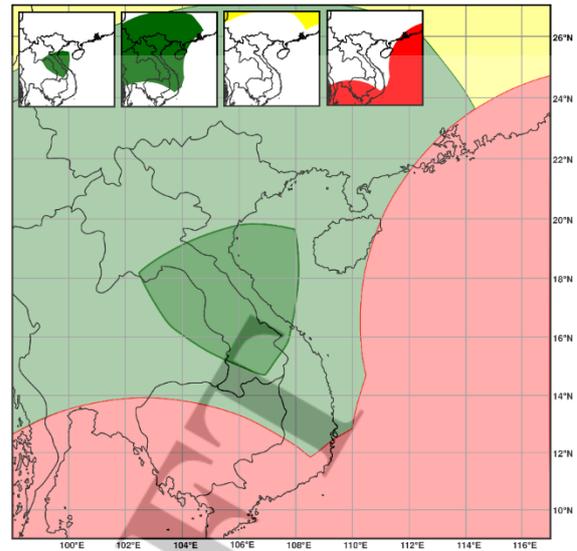
Fig. 2: A map utilizing data from the North American strewn field and comparing it with morphological groups of tektites in the Australasian region. All medial tektites (e.g., Philippinites) should be at least 930 km from the source crater, ruling out the areas in red. Medial tektite locations used: 16.386186° N, 119.892056° E, Bolinao, Philippines; 10.955550° N, 119.405150° E, northern Palawan, Philippines; 4.952386° N, 114.835486° E, Brunei; -2.923631° S, 108.206319° E, Belitung, Indonesia; 4.750000° N, 103.166667° E, Malay Peninsula, Malaysia. All proximal tektites (e.g., Indochinites) should be within 1,955 km of the source crater: possible areas are in green. If it is assumed that all proximal tektites occur within 930 km of the source crater (a number likely marginally too low) then the darker green area is the most probable crater location (in reality, this is almost certainly a broader area focused on this region as 930 km represents a minimum value). The yellow area is lower probability. Inset: Data used in map overlay. Green = Probable regions; Yellow = Less favorable regions; Red = Incompatible regions for the AAT impact.
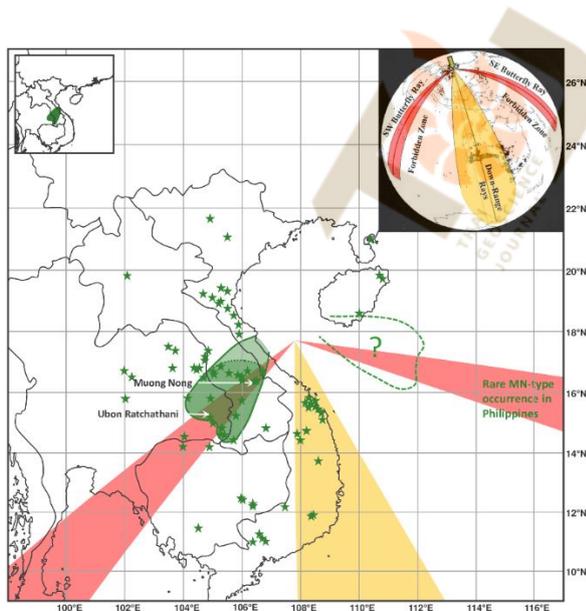
2.7 Distribution of MN-Type Layered Impact Glass: Muong Nong-type (MN-type) layered impact glasses are the lowest temperature ballistically (Huber, 2009; Koeberl, 1992; Schnetzler, 1992) ejected melts. These impact glasses are not entirely homogenized, are volatile-rich in comparison to tektites, may contain microscopic relict mineral grains, and have alternating layers of different composition (Koeberl, 1986). Logically, MN-type tektites are expected to occur in proximity to the source crater. A triangular wedge-shaped ~65,000 km^2 area was noted in northeastern Thailand, southern Laos, and central Vietnam where MN-type layered impact glasses occur in the absence (or near-absence) of true splash-form tektites (Fiske et

al., 1999; Schnetzler & McHone, 1996) (see **Fig. 3**). Further afield a mixture of MN-type layered impact glasses and splash-form tektites occur. Then further out, importantly in all directions, only splash-form tektites, in the absence of MN-type layered impact glasses, occur (**Fig. 3**). This triangular wedge-shaped area of MN-type layered impact glasses has been assumed by many to represent the center of the proximal tektite distribution and the impact crater should lie close by. However, this region of MN-type impact glasses is neither in the most northwesterly part of the strewn field nor in the center of the proximal splash-form tektite and MN-type impact glass distribution: instead, it is rather unsatisfactorily to the southwest of center.

The triangular wedge of MN-type layered impact glasses can be followed to the southwest (see **Fig. 3**) and it appears to be the proximal part of the prominent southwesterly butterfly ray. This ray extends into the central Indian Ocean and beyond, almost reaching the southernmost tip of Africa. The triangular wedge of MN-type layered impact glasses points towards an origin in the Gulf of Tonkin, possibly forming arcuate rays in a cardioid (heart)-shaped pattern, with reference to Schultz et al. (2009, 2007). A mirroring wedge of MN-type layered impact glasses would be

expected on the southeasterly butterfly ray that extends through northern Manila and Paracale in the Philippines, onwards in the direction of Micronesia in the southern Pacific Ocean. This mirroring wedge of MN-type layered impact glasses cannot be observed, if present, as it falls in the Gulf of Tonkin and South China Sea. In support of its presence, rare examples of MN-type layered impact glasses have been found along the same trajectory in Manila and Paracale in the Philippines (Chapman & Scheiber, 1969; Whymark, 2020). It is apparent, as seen in all oblique crater ray systems, that ejecta distribution is not equal. This scenario is depicted in **Fig. 3**.

Regardless of whether the triangular wedge-shaped area of MN-type layered tektites is accepted as the center of distribution or whether this region is accepted as the proximal part of the southwesterly butterfly ray, with the center of distribution in the Gulf of Tonkin, it is evident the lowest temperature melts are not concentrated in the most northwesterly area of tektite distribution (i.e., Yunnan and Guangxi regions of China and northern Vietnam) (**Fig. 4**). This observation is critical as it implies a crater located in the center of the proximal part of the strewn field and implies the presence of uprange ejecta.

Fig. 3: The distribution of MN-type layered impact glasses (green stars). The green region is predominantly MN-type layered impact glasses in the absence (or near-absence) of splash-form tektites (Fiske et al., 1999; Schnetzler & McHone, 1996). This region has traditionally been taken as the center of the Australasian strewn field. In fact, it may represent one of two butterfly rays emanating from the Gulf of Tonkin (suggested by green dashed line) (Whymark, 2020). The most prominent rays are indicated, with an assumed crater position in the Gulf of Tonkin as per Whymark (2013) (note that this location is not proven). Note how the green region of MN-type layered impact glass and prominent localities such as Muong Nong and Ubon Ratchathani lie beneath this inferred ray. Inset: Data used in map overlay. Green = Probable regions for the AAT impact.
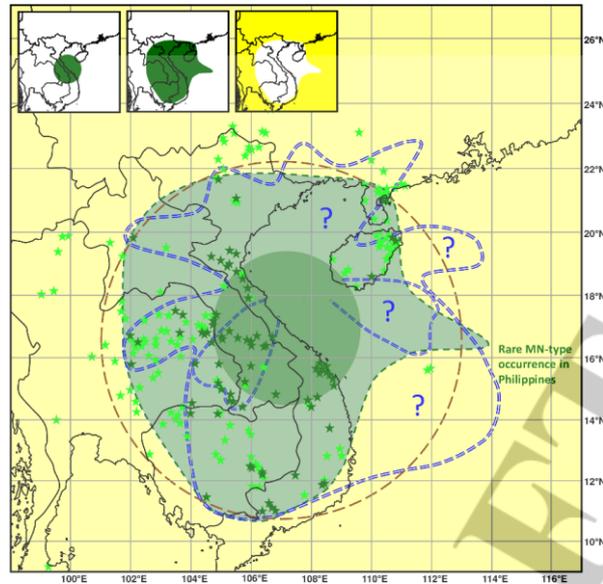
Fig. 4: Possible solutions for the distribution of MN-type layered impact glasses. Dark green stars represent MN-type layered impact glass occurrence. Bright green stars represent splash-form or undifferentiated tektite occurrence. Note how splash-form morphologies continue to occur at distance, surrounding the centrally located MN-type layered impact glasses. The outer limit of the observed distribution on MN-type layered impact glasses is shown by the dark green dashed line. The brown dashed line represents the circular best fit. The absence of data to the east and southeast leaves a degree of uncertainty as to the center of distribution. The presence of MN-type layered impact glass in the Philippines is suggestive that there is another triangular wedge of MN-type layered impact glass along the southeasterly butterfly ray in the Gulf of Tonkin and South China Sea. The triangular wedge of predominantly MN-type layered impact glass (Fiske et al., 1999; Schnetzler & McHone, 1996) is likely the proximal part of the southwesterly butterfly ray as opposed to the center of tektite distribution. This scenario is shown by the blue dashed line. Regardless of the precise scenario, the center of distribution likely lies somewhere in the darker green shaded region. The yellow area is lower probability. Inset: Data used in map overlay. Green = Probable regions; Yellow = Less favorable regions for the AAT impact.

2.8 Tektite Crater Rays: Ejecta rays can be seen emanating from craters on geologically less active planetary bodies (e.g., the Moon, Mercury, Ganymede). Increased gravity and increased atmospheric density (e.g., Venus) will act to suppress ejecta rays (Schultz, 1992). The Earth has slightly greater gravity than Venus but the atmosphere on Earth is significantly less dense. Tektite droplets, forming from the ejecta curtain at altitude, would be less inhibited on Earth, compared with Venus. The presence of distal AAT (e.g., Australites) that re-entered the atmosphere (Chapman, 1964) is proof that AAT ejecta was not wholly suppressed by the Earth's gravity and atmosphere. The distance that AAT ejecta has travelled, by comparison to crater rays on other planetary bodies, indicates that tektites are part of a crater ray system as opposed to randomly distributed.

In Australia, the prominent linear tektite concentration that runs through South Australia, Victoria, and into Tasmania has a distinct high calcium (HCa) geochemical profile (Chapman, 1971). The combined linear tektite distribution and distinct geochemistry indicate this feature is an ejecta ray. The presence of at least one AAT ejecta ray suggests the existence of a crater ray system. Tektite distribution patterns, in terms of location, abundance, and maximum tektite size, hint at a further two ejecta rays in Western Australia. In the Philippines, a prominent ray is suggested from Zambales, through northern Manila, Rizal Province (Tanay, Siniloan), Paracale, Catanduanes, and onwards into the Pacific Ocean. Notably, this ray yields the largest splash-form tektites in existence (Whymark, 2015). Further, less distinct, rays may be present in the Philippines. In the Malay Peninsula, an ejecta ray may be present but is not sufficiently distinct to confidently deduce an accurate azimuth. Microtektite distribution has been widely accepted to indicate two mirroring butterfly rays (Glass & Koeberl, 2006; Prasad et al., 2007). The southeast

butterfly ray extends from the northern Manila - Paracale region out into the Pacific Ocean towards Nauru. The southwest butterfly ray extends from the prominent Muong Nong-type layered impact glass localities of Muong Nong, Laos, and Ubon Ratchathani, Thailand, into the Indian Ocean to a region south of Madagascar.

Sufficient evidence exists from observation (e.g., Chapman, 1971; Dunn, 1912; Fenner, 1935) and from modelling (e.g., Artemieva, 2013) to indicate an uneven AAT distribution, in the form of ejecta rays, in medial and distal tektites and even possibly in the proximal setting (Izokh & An, 1983). A non-random tektite distribution implies that some tektite localities are related to one another (by means of occurring at different distances along the same ejecta ray). This theoretically allows for a best-fit impact location to be calculated. In doing so, stratigraphic outcrop bias (minimal in the young AAT ejecta); water transportation and redistribution (randomized on a global scale); the Coriolis effect (high tektite velocities (Chapman, 1964) result in minimal loft time); and post-impact plate tectonics, must be considered. Since the AAT impact, Australia is believed to have moved 54 km northwards with a slight clockwise rotation (B. C. Howard, 2016). These values become significant when regressing back thousands of kilometers and lead to a significant easterly shift in projections.

The use of a non-random tektite distribution pattern, corrected for the Coriolis effect and continental drift, should allow an accurate crater position to be calculated. This is beyond the scope of this article but is highlighted for future research to provide additional layers of data.

2.9 Microtektite Regression: Microtektites are found in the oceanic environment. Terrestrial microtektites, other than those in salt lakes or ice, are rapidly destroyed by dissolution in meteoric waters. Microtektite regressions therefore utilize a patchy distribution of distal oceanic borehole locations. Numerous microtektite regression studies have followed the same methodology but have progressively used a greater number of localities. The most recent study (Prasad et al., 2007), utilizing the greatest number of localities, is therefore the most accurate, superseding previous studies (see **Fig. 5**, large ellipse). The R^2 regression process was repeated using the same methodology and dataset from Prasad et al. (2007), but with a higher density mesh (0.25° spacing) to create a more detailed map and focal region (**Fig. 5**, small ellipse).
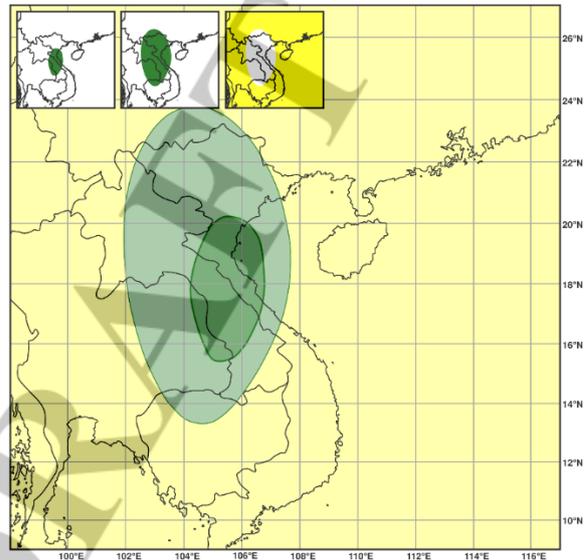
Fig. 5: An R^2 microtektite regression map based on 61 localities from Prasad et al. (2007) (light green). Utilizing identical methodology and dataset, but with a higher density of regression points, a focal point was calculated (dark green). The impact crater likely lies within the green region, with the darkest green region being most probable. The yellow area is lower probability. Inset: Data used in map overlay. Green = Probable regions; Yellow = Less favorable regions for the AAT impact.

Prasad et al. (2007) utilized 61 localities, of which only 15 were from the easterly portion of the strewn field and 46 from the westerly portion. The distance from the approximated source region also varied, with many easterly localities being more proximal. Ultimately, insufficient microtektite localities are available, particularly on the northern (continental) and eastern portion of the strewn field, to precisely locate the crater. A notable observation is that with increased microtektite localities the regressed crater location has varied quite considerably, and whilst becoming increasingly refined, the focal point of regression still has the possibility of readily shifting from its current location with the addition of new microtektite abundance data.

2.10 Target Lithology: Tektites, being a type of natural glass, require a network former (primarily silica), and therefore the source rock is necessarily a silica-rich rock. If the impactor strikes a silica-poor rock, then tektites cannot form. Terrestrial weathering processes act to concentrate silica in sedimentary rocks and their metamorphic descendants. Tektites form through shock melting so the temperature attained will be dependent on the compressibility of the rock: according to Stöffler, Hamann, & Metzler (2018) "…at a given shock pressure, the shock temperature of highly porous rocks can be up to an order of magnitude higher than those of dense crystalline rocks" (p. 2). Recently deposited water-rich siliciclastic sediments, common on the continental shelf, are therefore optimal for tektite production (K. T. Howard, 2011). Older siliciclastic sedimentary rocks are still suitable but are denser at surface (due to previous burial compaction) and so less compressible, followed by metamorphosed siliciclastic sedimentary rocks. Silica-rich igneous rocks, with low compressibility, could still form tektites but a much smaller volume of melt would attain sufficient temperature to fully melt.

Clues as to the tektite source material can be derived through the study of associated un-melted and partially melted lithologies, mineral grains in tektites and impact glasses (particularly in lower temperature melts), and through analysis of the geochemistry of fully melted tektites. Rock fragments recovered from the Australasian microtektite layer were found to be well sorted, quartz-rich, fine-grained (silt- to fine sand-sized) sedimentary rock (Glass & Barlow, 1979; Glass & Koeberl, 2006). A derivation from shales, graywackes, and lithic arenites has been suggested (Glass, Huber, & Koeberl, 2004; Koeberl, 1992). In agreement, K. T. Howard (2011) suggested a mixture of shale-like material and a very quartz-rich material. A minor carbonate (dolomite) component was suggested to explain the CaO (positively correlated with MgO) variation (Amare & Koeberl, 2006).

Coarse grained sedimentary rocks such as sandstones and conglomerates, as have been commonly described from Jurassic sediments in the central Indochinese region (Blum et al., 1992; Javanaphet, 1969; Sieh et al., 2020) (**Fig. 6**), are unsuitable source materials for AAT despite theoretically being suitable for tektite formation. This is further confirmed by REE analyses. Interlayered silts and shales may be suitable source materials, but not when considered in this heterogeneous context.
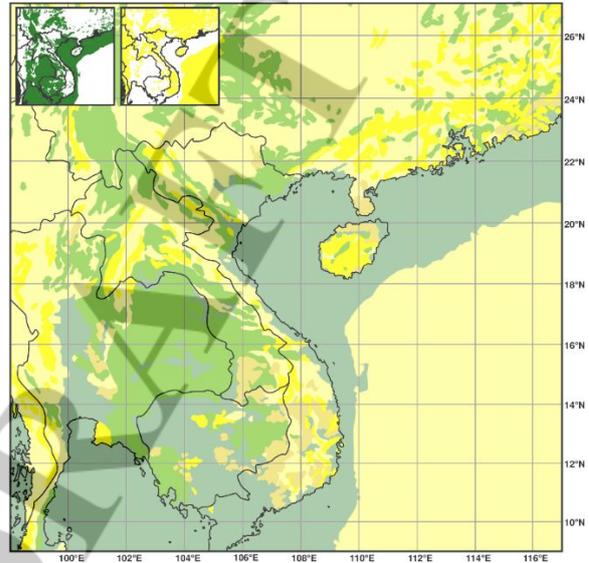

Fig. 6: A geological map outlining potentially suitable and unsuitable rock types for AAT. Mesozoic rocks (lime green), including Middle Jurassic strata. Quaternary outcrops and continental shelf areas (dull sea-green) which likely yield recent sediments. Green regions yield rocks of potentially suitable ages (dependent on various Rb/Sr and [10]Be interpretations) and may be compatible with the site of impact. Intrusive igneous rocks (bright yellow) are unlikely source materials and impact melts should not be surface exposed. Extrusive volcanic rocks (beige) are unlikely source regions due to geochemical incompatibility. Dull yellow regions represent outcropping rocks of incompatible age and incompatible deeper sea sediments. Yellow / beige regions have a low compatibility with the site of impact. After Liu et al. (2016). Inset: Data used in map overlay. Green = Probable regions; Yellow = Less favorable regions for the AAT impact.

Based on principal component analysis (PCA) using major-element tektite composition an admixture of sandstone and basalt was proposed by Sieh et al. (2020). As discussed in Section 2.15, thorough mixing is demonstrably poor in tektites (Glass & Simonson, 2013, p. 113; Koeberl, 1992). AAT REE data is incompatible with sandstone (**Fig. 7**) and basalt sources (**Fig. 8**) (Koeberl, 1992). Sr-Nd isotopic data is incompatible with

basalts (N. Hoang, Flower, & Carlson, 1996; N. Hoang, Hauzenberger, Fukuyama, & Konzett, 2018). PCA did, however, highlight compositional variations between early (distal) and late (proximal) formed tektites, reinforcing trends also seen in REE and Sr-Nd isotopes, indicative of a lithological variation with depth of excavation if a ballistic equivalent of 'inverted' stratigraphy is accepted. Igneous rocks as a target material are highly improbable from a geochemical (presented subsequently) and wide AAT distribution perspective. Impact-related melts should not be surface exposed in a recent impact that has suffered minimal erosion. Igneous provinces are improbable source regions (**Fig. 6**).

2.11 Rare-Earth Elements: Koeberl et al. (1985) states that rare-earth elements (REE) are known to be of "great genetic significance" (p. 108). REE are refractory elements, and their abundance pattern has not changed in the process of melting (Koeberl et al., 1985). Chondrite (McDonough & Sun, 1995) normalized REE patterns of averaged tektite values can be compared with various rock types. Koeberl et al. (1985) concluded that AAT '…follow very closely the pattern exhibited by the post-Archean upper crust average sediments and are very likely to have originated from such a source' p. 107. Averaged shale groupings (Condie, 1993; Howard, 2011; Koeberl et al., 1985; Lodders & Fegley, 1998), see **Fig. 7**, were highly comparable with AAT values. Graywacke values (Condie, 1993; Koeberl et al., 1985), see **Fig. 7**, conformed to the later stage splash-form and layered tektites. Sandstones (Condie, 1993; Koeberl et al., 1985), see **Fig. 7**, had low REE values, incompatible as a sole source for AAT.
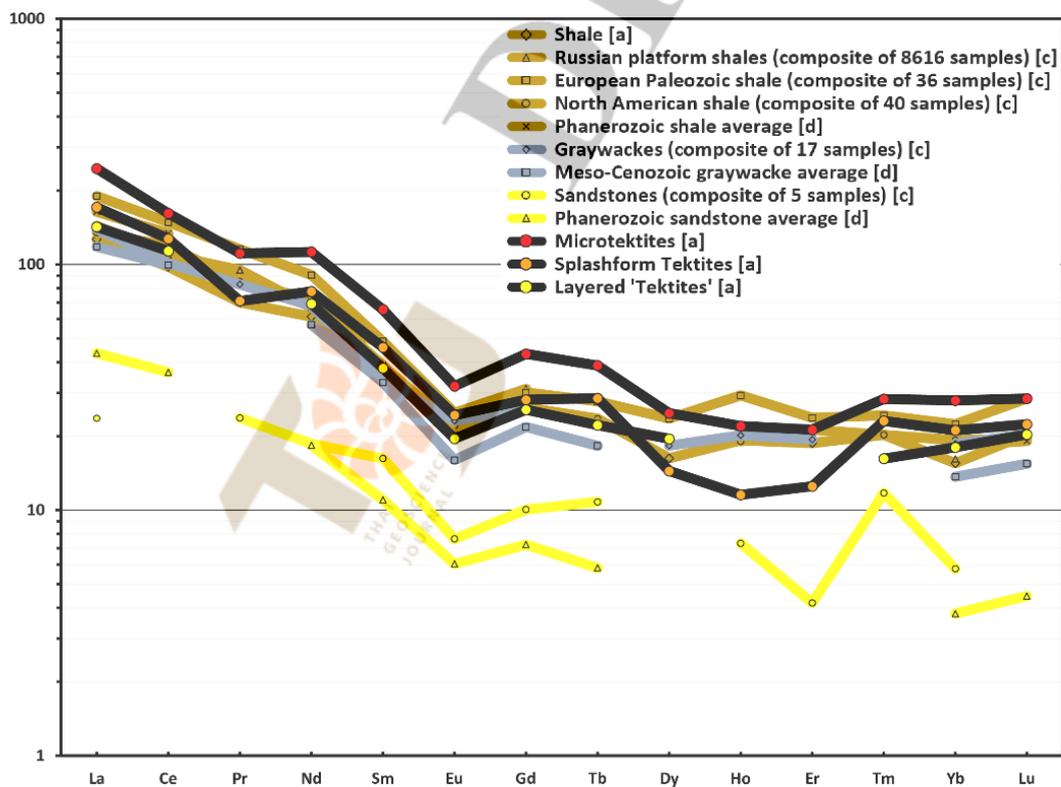
Fig. 7: Chondrite (McDonough & Sun, 1995) normalized rare-earth element patterns of average tektite values [a] (K. T. Howard, 2011) compared with shale, graywacke, and sandstone values. [a] K. T. Howard (2011) after Lodders & Fegley (1998); [c] Koeberl et al. (1985); [d] Condie (1993).
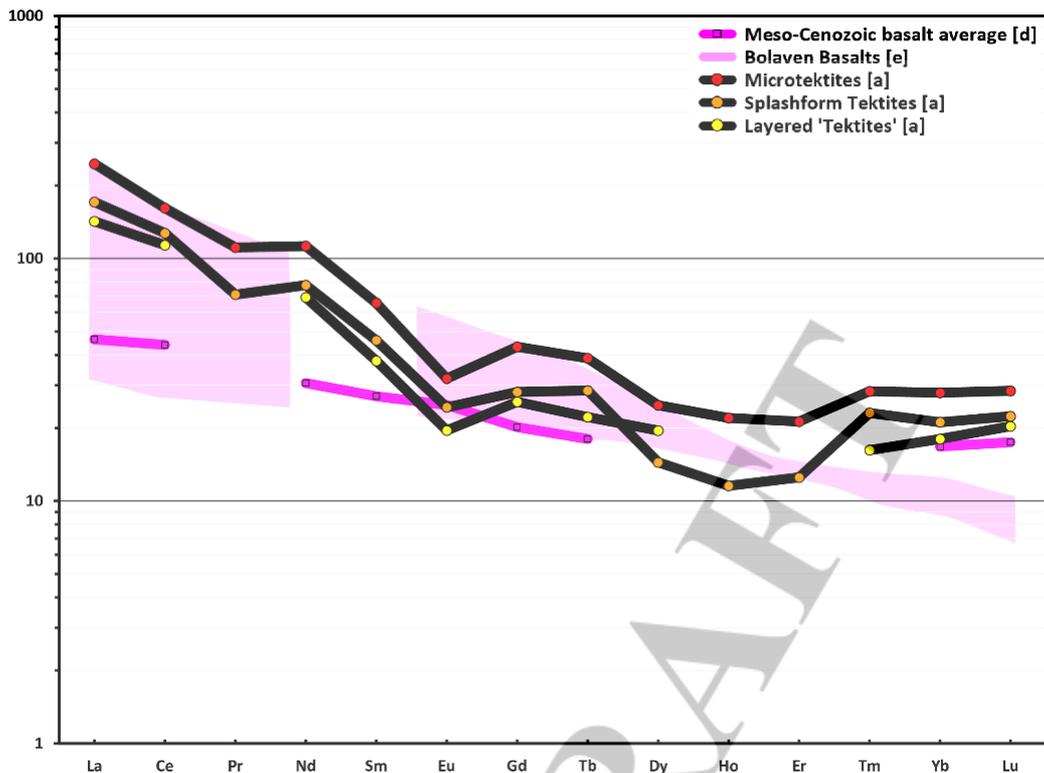
Fig. 8: Chondrite (McDonough & Sun, 1995) normalized rare-earth element patterns of average tektite values [a] (K. T. Howard, 2011) compared with Meso-Cenozoic basalt values: [d] Condie (1993). Various plotted Bolaven basalt compositions are duplicated from [e] N. Hoang et al. (2018).
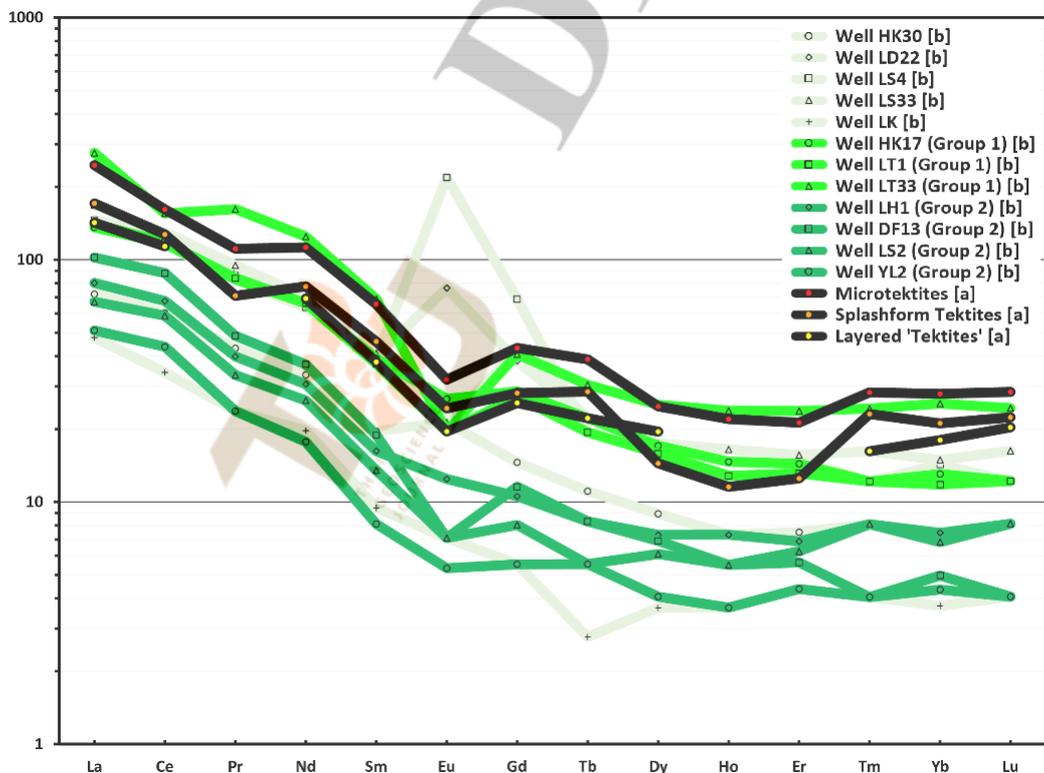
Fig. 9: Chondrite (McDonough & Sun, 1995) normalized rare-earth element patterns of average tektite values [a] (K. T. Howard, 2011) compared with Upper Miocene sediment values: [b] (Cao et al., 2015). Bright green wells were categorized by (Cao et al., 2015) as Group 1 wells with relatively high REE concentrations. Dark green wells were categorized by (Cao et al., 2015) as Group 2 wells with relatively low REE concentrations. Pale green wells were uncategorized, falling into both Group 1 and 2 with some anomalies.

REE values for basalt (including Bolaven Plateau basalts), see **Fig. 8**, did not reproduce the AAT REE pattern (Condie, 1993; N. Hoang et al., 2018). Basic igneous rocks can be excluded as a potential source material for AAT (wholly or in part) based on REE (N. Hoang et al., 1996, 2018; Koeberl, 1992) (**Fig. 8**). Koeberl (1992) states: 'Mixing of local soils, or with some related loess samples, cannot reproduce the tektite REE patterns, and any basaltic, oceanic, or extraterrestrial rocks can be excluded as source rocks…' p. 1033. **Figs. 7 & 8** demonstrate that REE patterns of sandstones and basalts, either in isolation or in combination, are incompatible with AAT.

All shales have similar REE patterns, so it is not possible to determine the exact precursor rock / formation from which AAT originated (Koeberl et al., 1985). It can simply be determined that the source rock was shale-rich and post-Archean (Koeberl et al., 1985). Averaged tektite values from K. T. Howard (2011), suggest that earlier formed microtektites have, on average, higher REE concentrations than splash-form tektites, which in turn have higher REE concentrations than the last formed layered 'tektites' (**Figs. 7 - 9**). If a ballistic equivalent of 'inverted' stratigraphy, a concept that is not proven but appears likely, is accepted then REE may indicate a subtle transition from shales to siltier / sandier interbedded shales or greywackes with greater depth of excavation.

Australasian tektite REE values can be compared with Upper Miocene sediments from boreholes in the Yinggehai Basin and Qiongdongnan Basin (Cao, Jiang, Wang, Zhang, & Sun, 2015), see **Fig. 9**. AAT REE values were comparable with sediments containing high REE concentrations, categorized as Group 1 wells by Cao et al. (2015). Average AAT microtektite values closely matched well LT33. Average AAT splash-form and layered 'tektite' values were comparable with wells HK17 and LT1, see **Fig. 9**. In the sparse data set, in terms of geographic and stratigraphic extent, Group 1 wells corresponded with regions surrounding Hainan, but notably no data for comparison is available offshore Vietnam. Sediments close to the Red River mouth and in central Qiongdongnan Basin showed low compatibility (**Figs. 9 & 10**). Cao et al. (2015) did not compare lithology to REE abundance. It is possible that compatible wells simply represent shale-rich sediments. Incompatible wells may represent sand-rich submarine or deltaic fans derived from rivers (**Fig. 10**). The most prominent river is the Red River which progrades into the northern part the Yinggehai - Song Hong (YGH-SH) Basin. Tektite REE data appears to preclude coarser siliciclastic sediment and, as such, may indicate a crater position away from a river mouth and its extended submarine fans.
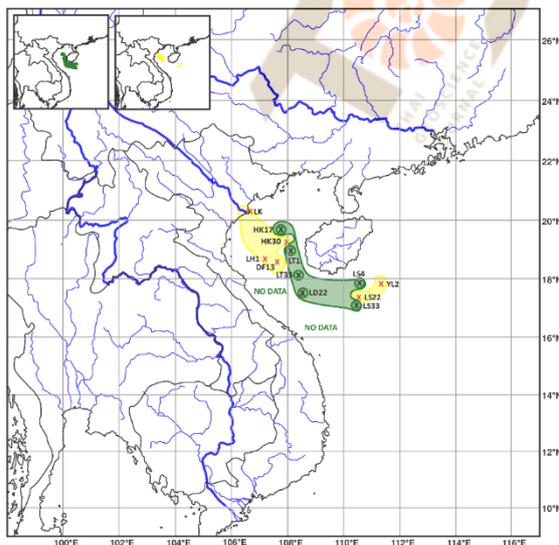
Fig. 10: REE compatibility of Upper Miocene sediments (Cao et al., 2015) with AAT (K. T. Howard, 2011). Wells with compatible Upper Miocene sediment are marked with a green circle and shaded green. Incompatible wells, likely representing sandier deposits, are marked with a red cross and shaded yellow. Stratigraphically results will vary. No data from Vietnamese wells. Modern rivers are depicted in blue, which are anticipated to deliver sand-rich sediments. Inset: Data used in map overlay. Green = Probable regions; Yellow = Less favorable regions for the AAT impact.

2.12 Strontium - Neodymium: Sr-Nd isotopic data can potentially be used to 'fingerprint' the source rock. As highlighted in Section 2.15, thorough mixing is demonstrably poor in tektites (Glass & Simonson, 2013, p. 113; Koeberl, 1992). The close grouping of Sr-Nd values in tektites (**Fig. 11**) would therefore be suggestive of a relatively homogenous target rock as opposed to thorough and efficient mixing of disparate melts (e.g., basalt and sandstone) in the brief seconds following impact. The constituents of fine-grained sedimentary rocks, identified as the probable source material (Section 2.10), are thoroughly mixed and homogenized by sedimentary transport processes resulting in consistency if derived from the same parent materials. **Fig. 11** demonstrates reasonably homogenized sediments in basins, versus the diversity in immature river sediments. In the suggested absence of thorough mixing of tektite melts a relatively homogenous source rock is interpreted.

Cross plots of $^{87}Sr/^{86}Sr$ against εNd values were constructed to compare published AAT values (Ackerman et al., 2020; Blum et al., 1992; Shaw & Wasserburg, 1982) with published river sediment data (Clift et al., 2008; Jonell et al., 2017; Liu et al., 2007) and with surface sediments of the South China Sea region (Wei et al., 2012), see **Fig. 11**. Slight differences in $^{87}Sr/^{86}Sr$ and εNd values between proximal and distal tektites are potentially indicative of derivation of tektites from variable depths in a stratified, but generically related, target (Blum et al., 1992). These data indicated a compatibility of AAT with sediments at the Red River mouth and the East Vietnam and South China Seas (see **Figs. 11 - 12**). Samples were not available in the Yinggehai - Song Hong (YGH-SH) Basin but modern-day Red River drainage accounts for approximately 80% the total sediment supply of the YGH-SH Basin (Feng et al., 2018). When sediment supply exceeded accommodation space in the YGH-SH Basin, the sediment 'spilled' into the East Vietnam and South China Seas. By inference, a YGH-SH Basin source, located between compatible sources and sinks, is likely compatible.
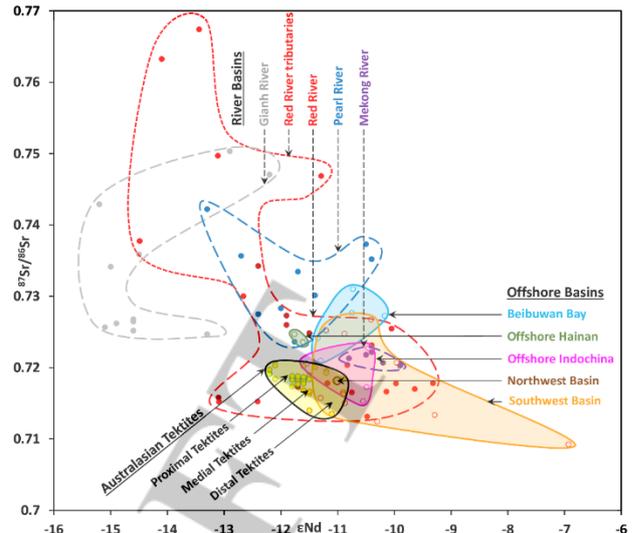
Fig. 11: Cross plot of Sr versus Nd isotope compositions of Australasian tektites and potential source materials from river basins and offshore basins. AAT overlap with Red River sediments, offshore Indochina, the Northwest Basin, and the Southwest Basin. No data was available for the YGH-SH Basin.
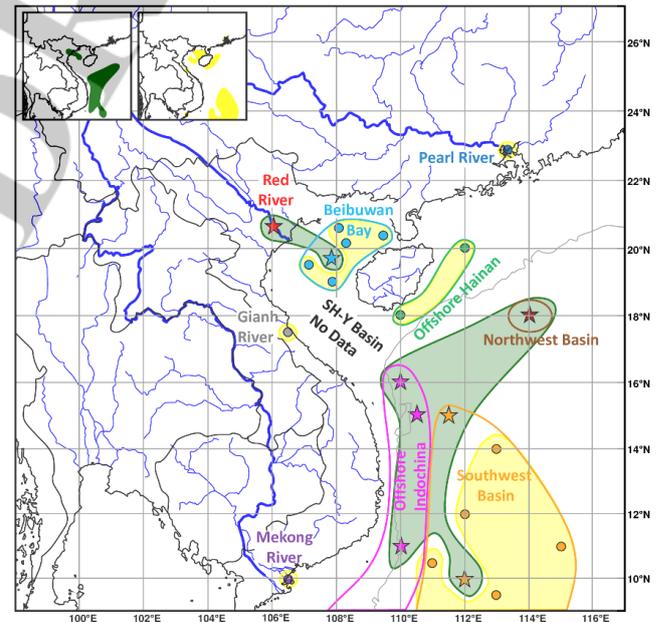
Fig. 12: Location of samples in cross plot (see **Fig. 11**) of Sr versus Nd isotope compositions for tektites (Ackerman et al., 2020; Blum et al., 1992; Shaw & Wasserburg, 1982) compared with basin sediments measured from offshore Hainan, Beibuwan Bay, offshore Indochina, Northwest Basin and Southwest Basin (Wei et al., 2012) and river sediments (Clift et al., 2008; Jonell et al., 2017; Liu et al., 2007). Samples with a star and green shaded areas are closely compatible with tektites. Samples denoted by a circle and yellow shaded areas indicate low compatibility with AAT. Modern rivers are depicted in blue. Inset: Data used in map overlay. Green = Probable regions; Yellow = Less favorable regions for the AAT impact.

Australasian tektite samples yielded εNd values between -10.9 and -12.2, averaging -11.58 (Ackerman et al., 2020; Blum et al., 1992; Shaw & Wasserburg, 1982). These consistent εNd values are indicative of a reasonably homogenous target material, or improbable scenario of a thoroughly mixed melt, from a single source crater. εNd values from the Red River mouth were -11.47 (Liu et al., 2007, 2016). AAT εNd values conformed closely with εNd values from the Red River mouth, YGH-SH Basin, Qiongdongnan Basin, Pearl River mouth and west Zhujiangkou Basin (fed by the Pearl River with Hainan influence). εNd values from the Mekong Delta did not match (-9.89 to -10.53) (Liu et al., 2007, 2016). εNd values were used to construct a map of potential source areas (see Fig. 13).

Fig. 13: Modern εNd values from (Liu et al., 2016). These values can be compared with tektite samples that yielded εNd values between -10.9 and -12.2, averaging -11.58 (Ackerman et al., 2020; Blum et al., 1992; Shaw & Wasserburg, 1982). Green areas represent suitable source areas. Yellow areas represent unlikely source areas. Inset: Data used in map overlay. Green = Probable regions; Yellow = Less favorable regions for the AAT impact.

Sr-Nd isotopic data of southern Vietnamese Basalts (N. Hoang et al., 1996) can be compared with tektites (Ackerman et al., 2020; Blum et al., 1992; Shaw & Wasserburg, 1982). In southern Vietnamese basalts $^{87}Sr/^{86}Sr$ values average 0.744 (0.7036 to 0.7065), compared to AAT that average 0.7169 (0.7118 to 0.7213); $^{143}Nd/^{144}Nd$ values average 0.5128 (0.5126 to 0.5130), compared to AAT that

average 0.5117 (0.5112 to 0.5121); εNd averages 3.72 (-0.9 to 7.6), compared to AAT that average -11.58 (-12.2 to -10.9) (Ackerman et al., 2020; Blum et al., 1992; N. Hoang et al., 1996; Shaw & Wasserburg, 1982). Values for Bolaven are not given, but $^{87}Sr/^{86}Sr$ and $^{143}Nd/^{144}Nd$ values of Bolaven basalts are plotted in N. Hoang et al. (2018) and fall centrally within the ranges of southern Vietnamese basalt values of N. Hoang et al. (1996). It is demonstrated that regional basalts are incompatible as a source material for AAT.

2.13 Major Element Geochemical Regression: The geographic distribution of SiO_2, Na_2O, and CaO concentrations in MN-type layered impact glasses and intermediate tektites are plotted from Schnetzler (1992) (**Figs. 14 - 16**). Schnetzler (1992) utilized a sparse data set with some approximated or poorly defined localities (SiO_2 = 22 localities / 166 analyses; Na_2O = 23 localities / 97 analyses; CaO = 24 localities / 98 analyses). The absence of data from the Gulf of Tonkin, East Vietnam Sea, and South China Sea potentially skews data westwards. Whilst trends are observed, the contours are somewhat subjective, and the possibility of erroneous localities cannot be dismissed. The use in map overlay, however, remains valid as the principle combines weak data to create a more robust argument through weight of evidence. The major element geochemical iso-concentrations in Schnetzler (1992) appear to trend to the center of the proximal tektite strewn field.

2.14 Beryllium-10 Regression: A trend of decreasing ^{10}Be content with proximity to the likely source area is observed (**Table 1**). This trend in ^{10}Be iso-concentrations within the AAT strewn field is increasingly being accepted as representing a ballistic equivalent of 'inverted' stratigraphy (Ma et al., 2004). An 'inverted' stratigraphy should be more evident if a thick sedimentary column has been sampled. ^{10}Be iso-concentrations of MN-type layered impact glasses were used by Ma et al. (2004) to calculate the crater position with the assumption that the crater would lie at the center of the lowest concentration of ^{10}Be (**Fig. 17**).

Fig. 14: The geographic distribution of SiO_2 concentrations in MN-type layered impact glasses and intermediate tektites based on 22 localities / 166 analyses (Schnetzler, 1992). Note the absence of data to the east and southeast due to the presence of seas. Green regions represent regions of higher probability and yellow areas denote lower probability for the presence of the AAT source crater. Inset: Data used in map overlay. Green = Probable regions; Yellow = Less favorable regions for the AAT impact.
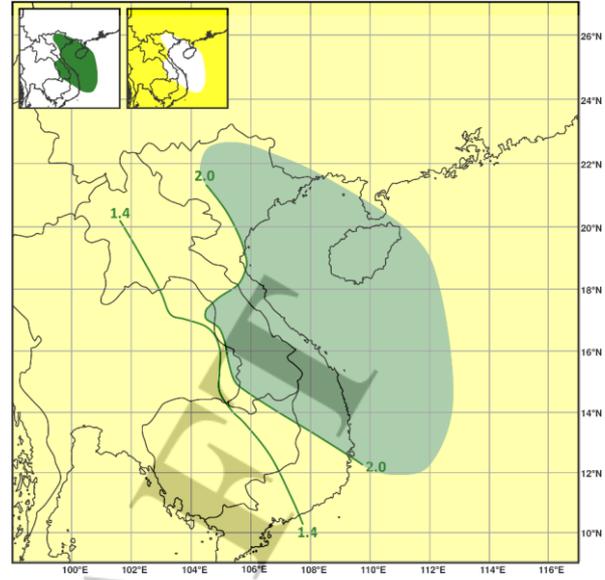
Fig. 16: The geographic distribution of CaO concentrations in MN-type layered impact glasses and intermediate tektites based on 24 localities / 98 analyses (Schnetzler, 1992). Note the absence of data to the east and southeast due to the presence of seas. Green regions represent regions of higher probability and yellow areas denote lower probability for the presence of the AAT source crater. Inset: Data used in map overlay. Green = Probable regions; Yellow = Less favorable regions for the AAT impact.
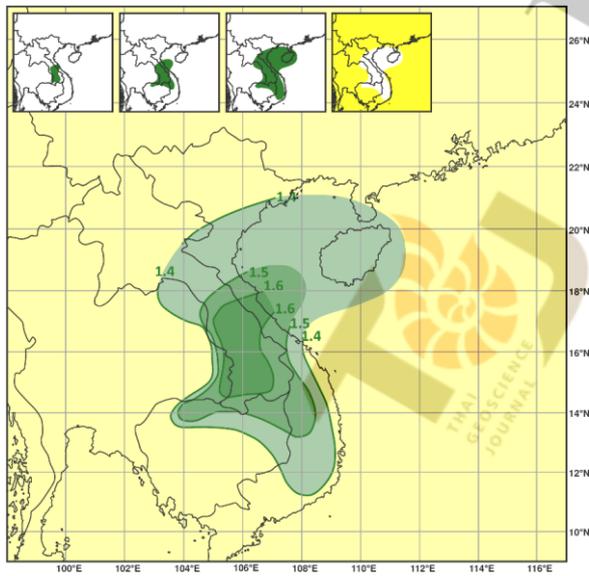
Fig. 15: The geographic distribution of Na_2O concentrations in MN-type layered impact glasses and intermediate tektites based on 23 localities / 97 analyses (Schnetzler, 1992). Note the absence of data to the east and southeast due to the presence of seas. Green regions represent regions of higher probability and yellow areas denote lower probability for the presence of the AAT source crater. Inset: Data used in map overlay. Green = Probable regions; Yellow = Less favorable regions for the AAT impact.
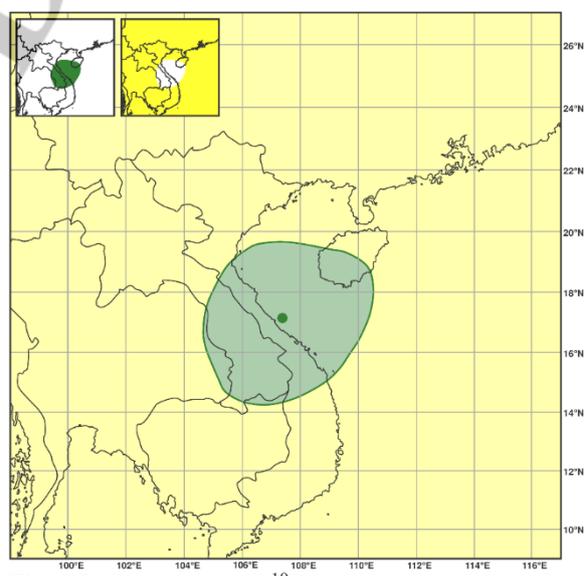
Fig. 17: Regression of [10]Be iso-concentrations (Ma et al., 2004) indicate the crater is within the shaded region, with the best fit at '•'. Note the absence of data to the east and southeast due to the presence of seas. The yellow shaded area denotes lower probability for the AAT source crater. Inset: Data used in map overlay. Green = Probable regions; Yellow = Less favorable regions for the AAT impact.

Table 1: Average ^{10}Be concentrations of tektites grouped by country. Sources: [1] = (Ma et al., 2004); [2] = (Rochette et al., 2018); [3] = (Koeberl, Nishiizumi, Caffee, & Glass, 2015). Note that corrections for *in situ* ^{10}Be production are minimal, not exceeding ~10×10^6 atom/g (Ma et al., 2004, after others).

Country	Average ^{10}Be (atoms/g)	Source
Laos	$59 \pm 9 \times 10^6$ (uncorrected)	[1]
Thailand	$71 \pm 17 \times 10^6$ (uncorrected)	[1]
Vietnam	$73 \pm 13 \times 10^6$ (uncorrected)	[1]
China	$85 \pm 24 \times 10^6$ (uncorrected)	[1]
Indonesia	$115 \pm 27 \times 10^6$ (uncorrected)	[1]
Philippines	$121 \pm 22 \times 10^6$ (uncorrected)	[1]
Australia	$136 \pm 30 \times 10^6$ (uncorrected)	[1]
Microtektites:		
Antarctica	$184 \pm 8 \times 10^6$ (corrected for *in situ* production)	[2]
S. China Sea	$260 \pm 60 \times 10^6$	[3]

2.15 Target Lithology Age: Rb-Sr versus ^{10}Be:

There is conflicting data regarding the stratigraphic age of the target material. Resolving this issue would significantly narrow down the crater search area. The conflicting data are:

- It was determined that the last major Rb-Sr fractionation event (i.e., weathering, transportation, and deposition) experienced by the sedimentary target materials occurred in a narrow range of stratigraphic ages ~170 Ma ago (Blum et al., 1992).
- The ^{10}Be content in tektites, half-life of 1.39 Ma (Chmeleff, Blanckenburg, Kossert, & Jakob, 2010; Korschinek et al., 2010), was recognized as being too high to be derived from a Middle Jurassic source rock (Blum et al., 1992). It was concluded by Ma et al. (2004) that the AAT source material "did not consist of older igneous or sedimentary rocks, but of unconsolidated materials or young sedimentary rocks" (p. 3887).

There are three solutions that might theoretically provide satisfactory outcomes (**Fig. 18**):

1) There is thorough mixing between Middle Jurassic rocks and a young surficial cover during melt production. If it were a young fluvial sediment cover a ~1:4 ratio of young fluvial sediment to Middle Jurassic rock (Blum et al., 1992) would be expected.

2) The source rock is solely Middle Jurassic in age. A weathered surface in the target area was exposed to meteoric waters for longer than the half-life of ^{10}Be and if ^{10}Be was not lost to erosion or solution then a ~200 m column of Middle Jurassic bedrock could yield the correct ^{10}Be content (Blum et al., 1992).

3) The source rock is a young unconsolidated sedimentary rock (Ma et al., 2004). This suggests that the Rb-Sr clock may not have been reset and represents the penultimate depositional cycle (at ~170 Ma) or an averaged Rb-Sr age (Cordani, Mizusaki, Kawashita, & Thomaz-Filho, 2004; Dickin, 2005).
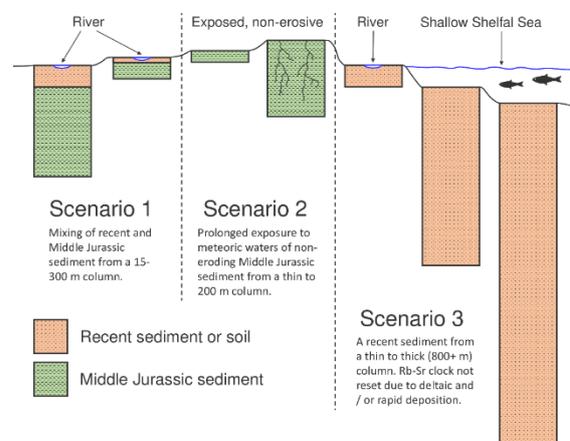
Fig. 18: Three scenarios that satisfactorily explain the Rb-Sr and ^{10}Be values.

Mixing is demonstrably poor in microtektites according to Glass & Simonson (2013): "There is not time for impact melt to be thoroughly mixed and homogenized prior to being ejected" (p. 113). Koeberl (1992) states that the lower temperature, MN-type layered impact glasses are "…compatible with incomplete mixtures of different target rocks" (p. 1056). It is assumed that microtektites represent early stage, typically shallow derived, melts whereas MN-type layered impact glasses represent later stage, on average more deeply excavated, melts. The compositional layering in MN-type impact glasses may reflect sedimentary bedding, indicative of melting with practically no mixing, implying [10]Be content at depth. It was remarked by Ma et al. (2004): "assuming that during crater formation neither the precursor grains nor the material melted mixed efficiently on a scale of tens of meters (N. A. Artemieva and E. Pierazzo, personal communication, 2002) we conclude that the vertical extent or thickness (as opposed to the absolute depth) of the hypothetical region that participated in tektite formation was likely between 15 and 300 m." (p. 3892).

The assumption made in Ma et al. (2004) was that if mixing is poor then high [10]Be values in tektite demonstrate a surficial origin (15 to 300 m). This has been supported by numerous authors: ~200 m (Blum et al., 1992); X0 m (Trnka, 2020); first tens of cm's of soil / sediment for Antarctica microtektites (Rochette et al., 2018). This assumption, however, is incorrect as it assumes an impact on land or in a region of normal sedimentation. Within the region of most probable impact (i.e., Indochinese to southern Chinese region) the YGH-SH Basin in the Gulf of Tonkin demonstrates exceptionally high sedimentation rates and therefore presumable abnormally high [10]Be content at great depth. Sediments predominantly comprise siliciclastic continental material in a deltaic to shallow marine setting. High [10]Be values in AAT do not demonstrate a surficial origin unless the source crater geology is known. [10]Be content does, however, potentially allow a crude understanding of stratigraphy at the unknown impact location if depth of excavation of tektites can be independently estimated.

Artemieva (2008) states that: "Excavation depth (initial position of ejecta in the target) drops quickly with increasing ejection velocity: from 0.25 Dpr for 2 km/s to 0.02 Dpr for 11 km/s" (p. 1) (Dpr = diameter of projectile). The trajectories of tektites, neglecting atmospheric drag, were calculated (Schmitt, 2004): at 2 km/s material is ejected laterally 204 km at 15° and 75°; 312 km at 25° and 65° to a maximum of 408 km at 45°. Moldavites, from Ries Crater, occur at distances beyond ~185 km. Assuming ejection angles from 15° to 75°, neglecting atmospheric drag, corresponding velocities of 1.35 to 1.9 km/s are calculated for these Moldavites, suggestive that tektites are present in ejecta travelling at under (or certainly close to) 2 km/s.

Atmospheric drag will, to varying degrees, raise the launch velocities required to eject a body a certain distance, in turn reducing the depth from which tektite could have been produced. In the early stages of impact, material is jetted (Vickery, 1993) and discrete tektite droplets form from the ejecta curtain at variable altitudes. The rarefied atmosphere is demonstrated by tektite bubble pressures (Matsuda, Maruoka, Pinti, & Koeberl, 1996; Mizote, Matsumoto, Matsuda, & Koeberl, 2003; Zähringer & Gentner, 1963). In larger impacts, such as the AAT impact, the influence of atmospheric drag is less prominent as the ejecta accelerates the atmosphere (Shuvalov & Dypvik, 2013). The large size of the AAT impact and the evidence of the formation of discrete tektite droplets at altitude significantly reduces, but does not eliminate atmospheric interaction, as manifested in the plastic deformation of tektite droplets, especially in proximal morphologies.

It is reasonable to assume that the AAT impact was comparable in size to the Chesapeake Bay impact (or possibly marginally larger), which is believed to have been produced by a 3.2 km diameter impactor (Kenkmann et al., 2009). An impactor of this diameter might excavate tektite producing ejecta to a depth of 800+ m, after Artemieva

(2008), assuming no / shallow seas and suitable glass-forming lithologies in the stratigraphy.

Three possible impact scenarios can now be presented:

A) The impact was a highly oblique grazing impact (< 5º) resulting in an elliptical crater. Consequently, tektites were only produced from surficial material.

B) The impact was oblique and resulted in a near-circular crater. However, tektites were only produced from the surficial layers as the strata at depth was incompatible with glass formation (e.g., limestone or anhydrite).

C) The impact was oblique and resulted in a near-circular crater. Tektites were produced from rock derived from the surface to ~800 m depth.

The arguments can be readily tested as the surficial (early stage) origin of tektites (A & B) necessitate that ejecta is predominantly downrange with a distinct uprange zone of avoidance (Gault & Wedekind, 1978; Schultz et al., 2009, 2007), i.e., an impact in northernmost Vietnam or Yunnan Province in China. Whereas C would eject tektites throughout the 360º azimuthal range (uprange and downrange) (Gault & Wedekind, 1978) with a crater in the center of the proximal strewn field (Ubon Ratchathani Province of Thailand, Savannakhét, Salavan, and Champasak Provinces of central-southern Laos, central Vietnam, and the Gulf of Tonkin).

Scenario A has been discussed and can be dismissed based on the azimuth of the butterfly lobes (Gault & Wedekind, 1978). Multiple parameters, including microtektite regression (Prasad et al., 2007), geochemical regression (Ma et al., 2004; Schnetzler, 1992), and MN-type layered impact glass distribution (Schnetzler, 1992) all point to a broadly central crater position either in the central-eastern part of Indochina or into the Gulf of Tonkin. This dictates that the proximal ejecta in this oblique impact is, in part, uprange and was therefore later stage, coming from depth as the circular crater opened-up. The observations of uprange AAT indicate the solution is Scenario C. Whilst tektites are typically considered

downrange ejecta, it is notable that the Chesapeake Bay Crater produced rare probable uprange ejecta at Martha's Vineyard (Burns, Schnetzler, & Chase, 1961).

Poorly mixed MN-type layered impact glasses are therefore assumed to be derived from up to ~800 m depth, after (Artemieva, 2008). The implication of high ^{10}Be values at depth in the presence of poor mixing, is that there is a thick sequence of recent sediments at the impact site. Some ballpark calculations for the impact site stratigraphy can be made if the ^{10}Be iso-concentrations are interpreted to represent a ballistic equivalent of 'inverted' stratigraphy. Assuming the impact was penecontemporaneous with sediment deposition, Antarctic, and South China Sea microtektites represent the first formed surficial ejecta, and tektites in Laos represent the last formed ejecta, a 2.28 to 2.97 Ma packet of sediment was sampled by AAT (early Pleistocene to Pliocene). Assuming ~800 m depth was sampled; an average sedimentation rate of 269 to 351 m/Ma is derived. The calculations are crude owing to multiple variables, but the principal point is that acceptance of uprange tektite distribution demonstrates excavation from depth and by inference a thick sequence of recent, rapidly deposited, sediment was sampled by AAT. Even if the sediment column estimate was reduced in consideration of atmospheric drag, the same conclusions will apply. Material is not ejected uprange until later stages of impact as the circular crater forms.

To reset the Rb-Sr clock substantial exchange and homogenization of Sr with sea / formation water is required. Rapidly deposited sediments, especially in a deltaic, but even in open marine environments, may preserve previous Rb-Sr dates (Cordani et al., 2004) / an average of the provenance ages of the sedimentary constituents (Dickin, 2005).

A very fine, almost authigenic, claystone comprising minerals such as illite, free from detrital minerals, is optimal to reset the Rb-Sr clock (Dickin, 2005). A low percentage of illite might be taken as an indicator that the region is unsuitable for resetting the Rb-Sr clock, and as such may indicate viability as a source crater

region (**Fig. 19**). In the YGH-SH Basin, clay mineral transformation, including illitization, typically occurs below 2,000 m sediment depth (Jiang, Xie, Chen, Wang, & Li, 2015). The uppermost 2,000 m of YGH-SH Basin sediment (deposited shortly before the impact and melted and ejected prior to illitization) would fulfil the ^{10}Be and Rb-Sr observations.
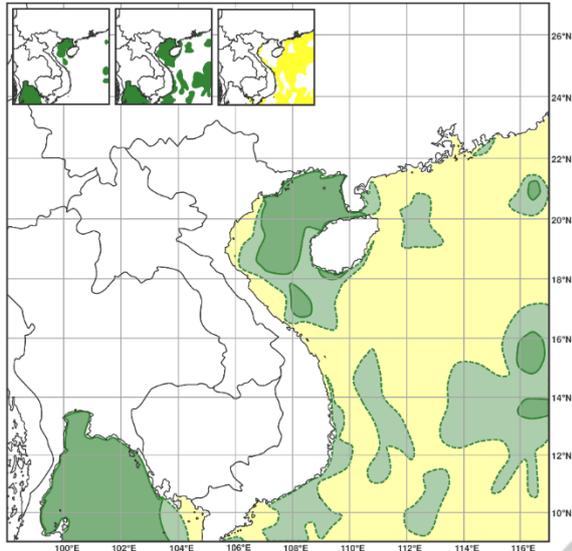
Fig. 19: Illite percentages in modern sediments after Liu et al. (2016). Solid lines with darker green shading represent under 20% illite. Dashed lines with lighter green shading represent under 30% illite. Yellow shaded regions yielded over 30% illite and represent lower probability regions. The Gulf of Tonkin region averages 27% illite. If it is assumed that the Rb-Sr clock was not reset, then areas of low illite concentrations represent plausible impact locations as these are the least suitable clay-rich rocks for obtaining a reset Rb-Sr age. Inset: Data used in map overlay. Green = Probable regions; Yellow = Less favorable regions for the AAT impact.

2.16 Pore Water / Sea Water Mixing Considerations: Tektites have very low water contents (Beran & Koeberl, 1997) due to the high formation temperatures that cause water to dissociate into H^+ and O^{-2} ions (Vickery & Browning, 1991). Ackerman, Skála, Křížová, Žák, & Magna (2019) believe that "volatile species derived from dissociated seawater and / or saline pore water" (p.179) may aid the loss of Os in the form of Os oxides. According to Ackerman et al. (2019) "The low Os abundance in most of the analyzed Australasian tektites, combined with non-radiogenic ^{187}Os/^{188}Os far below average upper continental crust, may provide a direct test to distinguish continental versus seawater impact scenario" (p. 179). The presence of significant amounts of water is envisaged in the formation of AAT (Ackerman et al., 2019). This work followed K. T. Howard (2011) who had noted that where tektites are present, a water-rich surface layer can be inferred. The abundance and widespread distribution of AAT necessarily implicates a water-rich target.

A saline character of the pore water is supported by the elevated halogen content of AAT (Ackerman et al., 2019; Koeberl, 1992; Meisel, Langenauer, & Krähenbühl, 1992). AAT were noted to have relatively high B and Li abundances and δ^{11}B values of (-4.9 to +1.4‰) (Chaussidon & Koeberl, 1995). The B, Li, and δ^{11}B values were indicative of a source rock with a higher clay content and are consistent with marine pelagic and neritic sediments as well as river and deltaic sediments (Chaussidon & Koeberl, 1995). ^{10}Be, Rb-Sr and Sm-Nd values were indicative of a continental crustal source rock (Blum et al., 1992) and eliminated pelagic and deeper neritic sediments (Chaussidon & Koeberl, 1995). It was concluded that AAT were derived from river and deltaic sediments with a higher clay content that have acquired B from the seawater (Chaussidon & Koeberl, 1995). Offshore Mekong River delta sediment was considered a potential source due to the rapid deposition rate of ^{10}Be-rich sediments (Chaussidon & Koeberl, 1995). A Mekong River source can now be eliminated by poorly compatible εNd values (Liu et al., 2007) and geographic position. The same conclusions, however, exceedingly accurately fit a Red River derived YGH-SH Basin source.

2.17 Sea Level in Source Region: The AAT impact occurred immediately prior to Termination IX, the transition from Marine Isotope Stage 19-20 (Mark et al., 2017). So, the impact occurred during a glacial stage when sea levels were low. Continental shelf regions, including the Gulf of Tonkin, would have been subaerially exposed, deltaic, or shallow shelf seas.

It is suggested that water-rich surface layers enhance, by orders of magnitude, the production of high velocity ejected melt (K. T.

Howard, 2011). Recently deposited, uncompacted, siliciclastic sediments have a much higher pore water content compared to mature sedimentary rocks exposed at the surface and are therefore optimal for tektite production.

It was modelled that an impact into 300 m water depth, compared to dry land, will result in a greater distribution of tektites (Artemieva, 2013). A 300 m water depth, however, would significantly curtail the production of the highest velocity distal ejecta, by reference to Artemieva (2008), which are notably present in abundance. With greater water depth the lithologies become geochemically (^{10}Be, Rb-Sr) less suitable. A water depth of tens of meters (or less) corresponding to a glacial lowstand on the continental shelf is likely to be realistic (**Fig. 20**). The source region might be broadly envisaged within the realm of a river delta to shallow shelf sea containing poorly compacted, rapidly deposited sediments with saline pore waters.
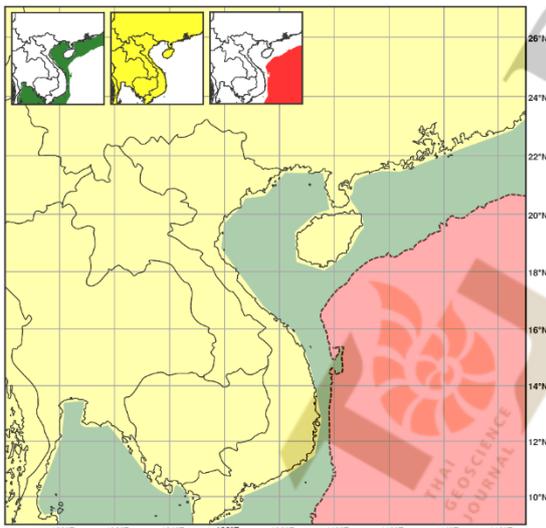
Fig. 20: The deeper seas in red cannot be considered as potential source areas as they could not produce the distal tektites. The areas in green are continental shelf regions (to 500 m below present sea level) (Liu et al., 2016). This shelf region is ideal for tektite production and some of this area would have been land during glacial lowstand. The area in yellow represents land areas which have a low probability of yielding the AAT source crater, simply because the crater would be evident and could not have been buried or eroded. Inset: Data used in map overlay. Green = Probable regions; Yellow = Less favorable regions; Red = Incompatible regions for the AAT impact.

2.18 Absence of Tsunamis Deposits: An impact on land or in a shallow sea would not be expected to produce significant tsunamis: resultant tsunamis would potentially be undifferentiable, in terms of magnitude, from tectonic tsunamis. Given the lower sea levels at the time of impact any evidence of tsunamis is likely below the current sea level.

2.19 Evidence of Cataclysmic Deposits: In northeastern Thailand tektite-bearing flood deposits have been reported from Ban Ta Chang (15.037° N, 102.291° E) and Chum Phuang (15.381° N, 102.728° E) (Bunopas et al., 1999). The presence of tektites and reversed polarities constrains the sediment to a period between the AAT impact event = 786 ± 2 ka (Mark et al., 2017) and the Brunhes / Matuyama polarity reversal = 783.4 ± 0.6 ka (Mark et al., 2017) (Haines, K. T. Howard, Ali, Burrett, & Bunopas, 2004; K. T. Howard, Haines, Burrett, Ali, & Bunopas, 2003). These catastrophic flood deposits are consistent with deposition shortly after the impact event. It is possible that these deposits are unrelated, but assuming that these deposits are related to the AAT impact event, it would suggest that the locations are within approximately 750 km of the impact site, after Collins, Melosh, & Marcus (2005).

2.20 Absence of a Crater: A recent crater that is 43 ± 9 km in diameter (Glass & Koeberl, 2006) is sought. A structure on land should form a distinctive morphological scar, which in tropical regions would be expected to form of a lake. The 1.83 km diameter, 0.576 Ma (±0.047 Ma), Lonar Crater (Jourdan, Moynier, Koeberl, & Eroglu, 2011; Schmieder & Kring, 2020) contains a 1.2 km diameter lake. The 10.5 km, 1.13 Ma (±0.10 Ma) (Jourdan, 2012; Koeberl, Bottomley, Glass, & Storzer, 1997; Schmieder & Kring, 2020) Bosumtwi Crater in Ghana, again in a tropical region, contains an 8 km diameter lake. The only significant lake in Indochina, Tonle Sap, was suggested as a possible source crater by Hartung & Koeberl (1994). Tektite distribution patterns and geochemical regressions would indicate that this cannot be the AAT source crater.

Given the absence of a lake, if the crater were onshore, it would be impossible to erode anything more than the most surficial part of a relatively pervasive impact structure. Distinct pyroclastic-like lithologies should be observed. Igneous-like lithologies would have been observed with deeper, but implausible, erosion. Estimated denudation rates are 23 m to 393 m since the AAT impact crater formed (Carter, Roques, & Bristow, 2000; Jonell et al., 2017; Yan, Carter, Palk, Brichau, & Hu, 2011) with perhaps ± 75 m of erosion being a realistic average value to use.

Destruction of the crater by tectonic processes can be ruled out in the brief time since impact. Tectonic processes may, however, have enhanced sediment accommodation space, assisting burial. Newly formed craters are natural depocenters. Furthermore, post-impact, the crater floor would be expected to continue to sag, e.g., Ries Crater experienced 134 +23/-49m of crater floor subsidence lasting more than 600 ka (Arp et al., 2021). Burial of the crater appears to be the only viable option to hide a crater.

Burial by extensive flood basalts is a possibility but would require a thick and extensive area of ~1,450 km^2 or more of post-impact age lava flows to cover a ~43 km diameter crater. Bolaven Plateau (seen in southern Laos in **Fig. 6**) is the only plausible (although sub-optimally placed) volcanic center in the region of interest. Bolaven lacks suitably extensive flood basalts of a young post-impact age, allowing, at best, a 17 km diameter crater (Sieh et al., 2020), which is 7 times less energetic than predicted, after Collins et al. (2005), and more comparable with the Bosumtwi impact that produced the much smaller Ivory Coast Tektite strewn field. Geochemical considerations have already been discussed and raise objections for an AAT impact into a pre-existing volcanic center.

Burial by sediments appears to be the only plausible option to hide a crater. This could be by river sediments or within a basin, such as the YGH-SH Basin (**Fig. 21**). A river scenario is somewhat problematic due to the raised crater rim geometry that would more likely result in a lake and diverted river system. A basin

scenario, with exceptionally high sedimentation rates, readily explains the absence of a crater and is entirely conceivable within the source region. Sedimentation rates in the YGH-SH Basin were estimated as 235 m/Ma in the late Miocene and 780 m/Ma in the Pliocene to Quaternary (Lei et al., 2011). High sedimentation rates prior to the impact readily explain the geochemical observations in tektites
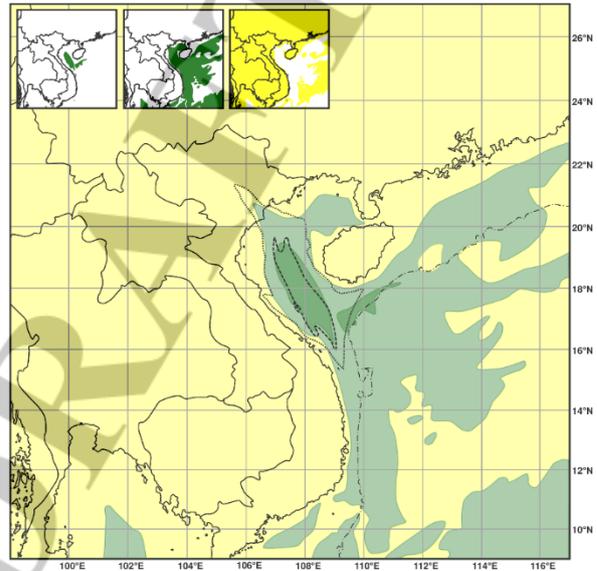

Fig. 21: Regions of moderate sedimentation rates (green) and high sedimentation rates (dark green), with a focus on Quaternary sedimentation (Métivier, Gaudemer, Tapponnier, & Klein, 1999). In terms of sedimentation, the dark green regions have, by far, the highest compatibility as a source region. Note that sedimentation rates and depocenters have varied considerably over time. The Yinggehai - Song Hong Basin is highlighted by a black dotted line with the depocenter marked by a black dashed line (Fan, 2018). The shelf break (500 m contour) is shown as a black dot-dashed line (Liu et al., 2016). Yellow shaded regions represent lower probability for the presence of the AAT impact crater. Inset: Data used in map overlay. Green = Probable regions; Yellow = Less favorable regions for the AAT impact.

2.21 Absence of an Ejecta Blanket: Whilst there have been reports of an ejecta blanket in and around the Bolaven Plateau (Sieh et al., 2020; Tada et al., 2019) (**Fig. 22**), no convincing evidence of a suevite deposits has been presented. The presence of high shock / high temperature tektites (Tada et al., 2019) in a low shock, un-melted, monomict breccia deposit suggests the crater is not nearby. The monolithologic, cobbly / boulder sandstone

breccia (Sieh et al., 2020; Tada et al., 2019) is unlike a proximal suevite, which characteristically yields partial melts. Furthermore, the single represented lithology is a sandstone, which is unsuitable from a REE perspective to be the AAT source material. A localized mass transport or flash flood origin might be more plausible, either unrelated to the AAT impact or (to explain a widespread occurrence) related in terms of devegetation in the impact aftermath. An ejecta blanket from a 43 km diameter crater would be expected to be 100 m thick at 16 km, 20 m thick at 43 km, 10 m thick at 60 km, 5 m thick at 81 km, and 1 m thick at 154 km from the rim of the post-impact crater. The described ejecta blanket is suggested to be 40-50 m thick (Sieh et al., 2020) based on the depth of incised stream valleys as opposed to direct observations. Tada et al. (2019) suggests an ejecta blanket ranging from under 1 m to a maximum of 9 m thickness. Sieh et al. (2020) models a much smaller impact of maximum 17 km diameter, which better fits with the proposed thinner ejecta blanket but fails to explain the widespread distribution and abundance of AAT. Finally, Sieh et al. (2020) elected not to perform a detailed study of planar deformation features in quartz grains, a diagnostic test (but not discounting reworking), instead relying on undiagnostic lithological observations of the deposit and the circular argument of proximity to an unproven crater. The proposed Bolaven ejecta blanket was not utilized in the map overlay, pending further evidence.

Tada et al. (2019) noted in their poster that the AAT proximal ejecta blanket has never conclusively been identified on land in Indochina. This observation remains true. Tada et al. (2019) went on to note that the ejecta deposit is important to constrain the impact location. Indeed, the absence of an ejecta blanket may be a constraining factor. It is difficult to envisage that all traces of an ejecta blanket have been eroded away. A more plausible explanation for the apparent absence of an ejecta blanket, is that the thick proximal ejecta deposit is located offshore (**Fig. 22**). If only a thin ejecta blanket was present onshore, then it is realistic that it could have been

entirely eroded or reworked. The absence of an ejecta blanket suggests the point of impact is far from the current shoreline: probably at least 50 km (as conservatively depicted in **Fig. 22**), and more likely over 80 km (resulting in up to a 42 m and 10 m thick ejecta layer, respectively, on the current land surface, pre-erosion).
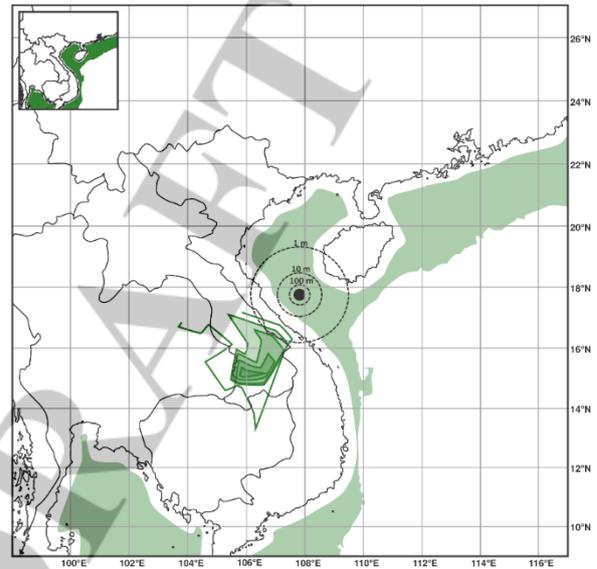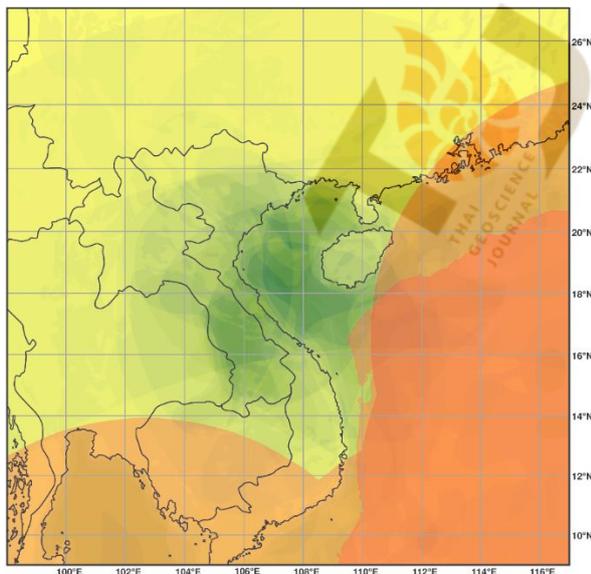

Fig. 22: Expected ejecta thickness from a 43 km diameter crater (black dashed lines). The crater position (Whymark, 2013) is for example only as the crater location is not established. In consideration of the absence of an ejecta layer onshore (either patchy or continuous), there is a higher probability that the impact was, conservatively, at least 50 km offshore from the current coastline (and likely more). A continental shelf region over 50 km from the current shoreline is depicted as a green shaded area. An unconfirmed ejecta layer was identified (Tada et al., 2019) (green lines centered on southern Laos). The breccia layer (Unit 2) reached a maximum thickness of 9 meters in the Bolaven Plateau. This unconfirmed ejecta layer was not utilized on composite overlay maps. Inset: Data used in map overlay. Green = Probable regions for the AAT impact.
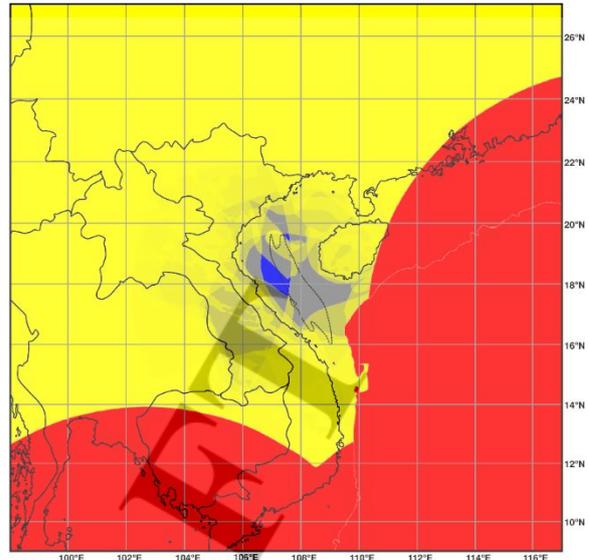
3. Conclusions

Multiple lines of independent data indicate that the AAT source crater will be found in the Gulf of Tonkin to central-eastern Indochinese region as opposed to ~800 km further north-northwest as would be implied if all tektites were downrange ejecta. Accepting a Gulf of Tonkin to central-eastern Indochina source region implies the existence of uprange tektites. The AAT impact was unarguably oblique, and as such there should be a distinct uprange zone of avoidance in the early phase

of impact (Gault & Wedekind, 1978; Schultz et al., 2009, 2007). Consequently, uprange tektites must be from a marginally later stage of impact. With reference to the calculated AAT crater diameter of 43 ± 9 km (Glass & Koeberl, 2006) and to ejection velocities in Artemieva (2008) it must be assumed that the uprange ejecta, for it to be present, must be deeply excavated. From the [10]Be content of these uprange tektites it must be concluded that a thick sequence of recent sedimentary rock has been sampled. This is indicative that the impact occurred in a pre-existing depocenter. The source crater location is thus largely restricted to the Song Hong-Yinggehai (YGH-SH) Basin. A YGH-SH Basin impact is not only in keeping with all available data, but the young, rapidly deposited, water saturated, siliciclastic sediment with saline formation water / seawater readily explain the abundance and geographic extent of the AAT. Furthermore, continued exceptionally high sedimentation rates in accommodation space created, in part, by the impact itself and subsequent sagging, would have resulted in rapid burial of the crater by hundreds of meters of sediment, thus explaining the apparent absence of the AAT source crater and its thick proximal ejecta blanket.

Fig. 24: Combined negative data for source crater location utilizing 50% transparency with a contrasting background color (blue). The dashed line represents the depocenter of the YGH-SH Basin. Blue areas = higher probability (no, or fewer objections). Yellow areas = lower probability. Red areas = no probability.

The principles of map overlay (McHarg, 1969) can be utilized to combine data and determine the most probable location of the AAT source crater. Some of the data presented and utilized is conflicting, e.g., the Jurassic versus recent (Rb/Sr versus [10]Be) age of the source rock. With perfect data sets all overlay map evidence will overlap on a central point. With more patchy or ambiguous data the overlap becomes partial or overlay elements become isolated, indicative that at least one of the lines of evidence is incorrect or insufficiently resolved. The nature of the partial data set for tektites, most critically for proximal tektites in the Gulf of Tonkin and South China Sea region, will result in error and a degree of skewness of the data. The use of multiple lines of evidence means that each observation only comprises a small percentage of the data set. Potentially misleading data should be overwhelmed by the weight of data, which, on average, should be correct.

An overlay map was constructed by placing maps of the same scale on top of one another. **Fig. 23**, constructed from all positive and negative data, utilized a total of 42 overlays (25 green, 15 yellow, and 2 red) taken from the insets in **Figs. 1 - 6, 10, 12 - 17, & 19 - 22**.

Fig. 23: Combined positive and negative data for source crater location. Greener areas = higher probability. Yellower areas = lower probability. Red / orange areas = no probability.

White (no data) regions were transparent, green and yellow data regions were 90% transparent, whilst red data was weighted at 70% transparency. The green shaded areas = higher probability, yellow shaded areas = lower probability, and red / orange shaded areas = no probability for the crater being in the region. **Fig. 24**, utilized only negative data, using 17 overlays (15 yellow, and 2 red) taken from the insets in **Figs. 1, 4 - 6, 10, 12 - 17, & 19 - 21**. White (no data) regions were transparent, yellow data regions were 50% transparent and red data was opaque. A blue background was added to highlight the most probable region of impact (blue). A region in the center or northwest segment of the Gulf of Tonkin had the least objections as an impact location, with a broader swathe encompassing the Gulf of Tonkin and central-eastern Indochina being plausible (**Figs. 23 & 24**). The most probable impact location, considering positive and negative data, is within ~100 km of E107.20°, N18.30°, but not (significantly) in a landward direction. The likelihood that the impact occurred in a depocenter with high sedimentation rates would indicate a basinward impact location (see **Fig. 24** for the YGH-SH Basin depocenter).

A possible structure exists in the YGH-SH Basin at E107.85°, N17.78° (Whymark, 2013, 2018). This depocenter region is known as the 'Great Sag' (Clift & Sun, 2006). Evidence of the presence of a crater include a 43 km diameter annular gravity anomaly (Whymark, 2013, 2018). A circular region of shallow-rooted chaotic seismic from approximately the time of impact to the late Miocene (Gong & Li, 2004; Gong et al., 1997; Yan et al., 2011). A circular pattern of shale diapirs (Lei et al., 2011, 2015) which may relate to post-impact geothermal activity conducting fluids along lines of weakness. An outer elliptical pattern of shale diapirs, possibly indicating significant slumping of the suspected crater, as would be anticipated from an oblique impact crater with asymmetrical depth profile in a continental shelf setting. A high geothermal gradient (Lei et al., 2011) may record the residual heat from the impact event. Seismic line 0755 (Lei et al., 2015, Fig. 3) (supported by Figs. 1.3.2.6 &

1.3.2.7 in CCOP, 2008) is apparently consistent with an impact crater (onlap, rim fault, and chaotic seismic). Further seismic lines have been recorded over the potential crater (Lei et al., 2015; CCOP, 2008) but are of poor resolution or are not in the public domain. Overlay of YGH-SH Basin geophysical and well data would narrow the search for the AAT source crater. Efforts to locate the AAT source crater must shift from improbable and fruitless onshore regions to the highly probable YGH-SH Basin.

Acknowledgments

Note

The author remains neutral regarding jurisdictional claims in maps and geographic nomenclature

References

Ackerman, L., Skála, R., Křížová, Š., Žák, K., & Magna, T. (2019). The quest for an extraterrestrial component in Muong Nong-type and splash-form Australasian tektites from Laos using highly siderophile elements and Re-Os isotope systematics. *Geochimica et Cosmochimica Acta, 252*, 179–189. https://doi.org/10.1016/j.gca.2019.03.009

Ackerman, L., Žák, K., Skála, R., Rejšek, J., Křížová, Š., Wimpenny, J., & Magna, T. (2020). Sr-Nd-Pb isotope systematics of Australasian tektites: Implications for the nature and composition of target materials and possible volatile loss of Pb. *Geochimica et Cosmochimica Acta, 276*, 135–150. https://doi.org/10.1016/j.gca.2020.02.025

Amare, K., & Koeberl, C. (2006). Variation of chemical composition in Australasian tektites from different localities in Vietnam. *Meteoritics & Planetary Science, 41*(1), 107–123. https://doi.org/10.1111/j.1945-5100.2006.tb00196.x

Arp, G., Dunkl, I., Jung, D., Karius, V., Lukács, R., Zeng, L., … Head III, J. W. (2021). A volcanic ash layer in the Nördlinger Ries impact structure (Miocene, Germany): Indication of crater fill geometry and origins of long-term crater floor sagging. *Journal of Geophysical Research: Planets*, e2020JE006764. https://doi.org/10.1029/2020JE006764

Artemieva, N. A. (2008, March 10–14). *Tektites: Model Versus Reality* [Abstract #1651]. Abstract submitted to the 39th Lunar and Planetary Science

Conference, League City, Texas, United States of America. Retrieved from: https://www.lpi.usra.edu/meetings/lpsc2008/pdf/1651.pdf

Artemieva, N. A. (2013, March 18–22). *Numerical Modeling of the Australasian Tektite Strewn Field* [Abstract #1410]. Abstract submitted to the 44th Lunar and Planetary Science Conference, The Woodlands, Texas, United States of America. Retrieved from: https://www.lpi.usra.edu/meetings/lpsc2013/pdf/1410.pdf

Artemieva, N. A., & Pierazzo, E. (2003, February 7-9). *Oblique Impact and its Ejecta: Numerical Modeling* [Abstract #8022]. Abstract submitted to: Impact Cratering, Bridging the Gap Between Modeling and Observations, Houston, Texas, United States of America. Retrieved from: https://www.lpi.usra.edu/meetings/impact2003/pdf/8022.pdf

Beran, A., & Koeberl, C. (1997). Water in tektites and impact glasses by fourier-transformed infrared spectrometry. *Meteoritics & Planetary Science, 32*(2), 211–216. https://doi.org/10.1111/j.1945-5100.1997.tb01260.x

Blum, J. D., Papanastassiou, D. A., Koeberl, C., & Wasserburg, G. J. (1992). Neodymium and strontium isotopic study of Australasian tektites: New constraints on the provenance and age of target materials. *Geochimica et Cosmochimica Acta, 56*(1), 483–492. https://doi.org/10.1016/0016-7037(92)90146-A

Bunopas, S., Wasson, J. T., Vella, P., Fontaine, H., Hada, S., Burrett, C., … Khositanont, S. (1999). Early Quaternary global terrestrial impact of a whole comet in the Australasian tektite field, newest apparent evidences discovery from Thailand and East Asia. *Bull. Geol. Soc. Malaysia. Proceedings Geosea '98 Ninth Regional Congress on Geology, Mineral and Energy Resources of Southeast Asia., 43,* 555–575. https://doi.org/10.7186/bgsm43199956

Burns, C. A., Schnetzler, C. C., & Chase, J. N. (1961). Tektite from Martha's Vineyard, Massachusetts. *Geological Society of America Bulletin, 72*(2), 339. https://doi.org/10.1130/0016-7606(1961)72[339:TFMVM]2.0.CO;2

Čada, M., Houzar, S., Hrazdil, V., & Skála, R. (2002, September 23-26). *Field Trip Guidebook and Abstracts*. Presented at the 9th International Conference on Moldavites, impact glasses and impact processes, Františkovy Lázně, Czech Republic.

Cao, L., Jiang, T., Wang, Z., Zhang, Y., & Sun, H. (2015). Provenance of Upper Miocene sediments in the Yinggehai and Qiongdongnan basins, northwestern South China Sea: Evidence from REE, heavy minerals and zircon U–Pb ages. *Marine Geology, 361*, 136–146. https://doi.org/10.1016/j.margeo.2015.01.007

Carter, A., Roques, D., & Bristow, C. S. (2000). Denudation history of onshore central Vietnam: Constraints on the Cenozoic evolution of the western margin of the South China Sea. *Tectonophysics, 322*(3–4), 265–277. https://doi.org/10.1016/S0040-1951(00)00091-3

CCOP (2008). Capacity Building within Geoscience in East and Southeast Asia Project (ICB-CCOP 1). *Final Report (Volume I) (p. 250). Bangkok, Thailand: Coordinating Committee for Geoscience Programmes in East and Southeast Asia (CCOP)*. Retrieved from: http://library.dmr.go.th/Document/DMR_Technical_Reports/2008/22539.pdf

Chapman, D. R. (1964). On the unity and origin of the Australasian tektites. *Geochimica et Cosmochimica Acta, 28*(6), 841–880. https://doi.org/10.1016/0016-7037(64)90036-5

Chapman, D. R. (1971). Australasian tektite geographic pattern, crater and ray of origin, and theory of tektite events. *Journal of Geophysical Research, 76*(26), 6309–6338. https://doi.org/10.1029/JB076i026p06309

Chapman, D. R., & Scheiber, L. C. (1969). Chemical investigation of Australasian tektites. *Journal of Geophysical Research, 74*(27), 6737–6776. https://doi.org/10.1029/JB074i027p06737

Chaussidon, M., & Koeberl, C. (1995). Boron content and isotopic composition of tektites and impact glasses: Constraints on source regions. *Geochimica et Cosmochimica Acta, 59*(3), 613–624. https://doi.org/10.1016/0016-7037(94)00368-V

Chmeleff, J., Blanckenburg, F. von, Kossert, K., & Jakob, D. (2010). Determination of the ^{10}Be half-life by multicollector ICP-MS and liquid scintillation counting. *Nuclear Instruments and Methods in Physics Research Section B: Beam Interactions with Materials and Atoms, 268*(2), 192–199. https://doi.org/10.1016/j.nimb.2009.09.012

Clift, P. D., Long, H. V., Hinton, R., Ellam, R. M., Hannigan, R., Tan, M. T., … Duc, N. A. (2008). Evolving east Asian river systems reconstructed by trace element and Pb and Nd isotope variations in modern and ancient Red River-Song Hong sediments: Evolution of East Asian River Systems. *Geochemistry, Geophysics, Geosystems, 9*(4). https://doi.org/10.1029/2007GC001867

Clift, P. D., & Sun, Z. (2006). The sedimentary and tectonic evolution of the Yinggehai-Song Hong basin and the southern Hainan margin, South China Sea: Implications for Tibetan uplift and monsoon intensification: Evolution of Yinggehai-Song Hong Basin. *Journal of Geophysical Research: Solid Earth, 111*(B6), B06405. https://doi.org/10.1029/2005JB004048

Collins, G. S., Melosh, H. J., & Marcus, R. A. (2005). Earth impact effects program: A web-based computer program for calculating the regional

environmental consequences of a meteoroid impact on Earth. *Meteoritics & Planetary Science, 40*(6), 817–840. https://doi.org/10.1111/j.1945-5100.2005.tb00157.x

Collins, G. S., & Wünnemann, K. (2005). How big was the Chesapeake Bay impact? Insight from numerical modeling. *Geology, 33*(12), 925–928. https://doi.org/10.1130/G21854.1

Condie, K. C. (1993). Chemical composition and evolution of the upper continental crust: Contrasting results from surface samples and shales. *Chemical Geology, 104*(1–4), 1–37. https://doi.org/10.1016/0009-2541(93)90140-E

Cordani, U. G., Mizusaki, A. M., Kawashita, K., & Thomaz-Filho, A. (2004). Rb–Sr systematics of Holocene pelitic sediments and their bearing on whole-rock dating. *Geological Magazine, 141*(2), 233–244. https://doi.org/10.1017/S0016756803008616

Dickin, A. P. (2005). *Radiogenic Isotope Geology* (2nd ed.), 492 p. Cambridge University Press. https://doi.org/10.1017/CBO9781139165150

Elkins-Tanton, L. T., Kelly, D. C., Bico, J., & Bush, J. W. M. (2002, March 11–15). *Microtektites as vapor condensates, and a possible new strewn field at 5 Ma* [Abstract #1622]. Abstract submitted to the 33rd Lunar and Planetary Science Conference, League City, Texas, United States of America. Retrieved from: https://www.lpi.usra.edu/meetings/lpsc2002/pdf/1622.pdf

Elliott, J. R., Huang, Y.-H., Minton, D. A., & Freed, A. M. (2018). The length of lunar crater rays explained using secondary crater scaling. *Icarus, 312*, 231–246. https://doi.org/10.1016/j.icarus.2018.04.015

Fan, C. (2018). Tectonic deformation features and petroleum geological significance in Yinggehai large strike-slip basin, South China Sea. *Petroleum Exploration and Development, 45*(2), 204–214. https://doi.org/10.1016/S1876-3804(18)30024-7

Feng, Y., Zhan, W., Chen, H., Jiang, T., Zhang, J., Osadczuk, A., … Zhang, W. (2018). Seismic characteristics and sedimentary record of the late Pleistocene delta offshore southwestern Hainan Island, northwestern South China Sea. *Interpretation, 6*(4), SO31-SO43. https://doi.org/10.1190/INT-2018-0012.1

Fenner, C. (1935). Australites, part II. Numbers, forms, distribution and origin. *Transactions of the Royal Society of South Australia, 59*, 125–140.

Fiske, P. S., Schnetzler, C. C., Mchone, J., Chanthavaichith, K. K., Homsombath, I., Phouthakayalat, T., … Xuan, P. T. (1999). Layered tektites of southeast Asia: Field studies in central Laos and Vietnam. *Meteoritics & Planetary Science, 34*(5), 757–761. https://onlinelibrary.wiley.com/doi/abs/10.1111/j.1945-5100.1999.tb01388.x

Gault, D. E., & Wedekind, J. A. (1978, March 13-17). *Experimental studies of oblique impact*. In: Proceedings of the 9th Lunar and Planetary Science Conference (pp. 3843-3875), Houston, Texas, United States of America. Retrieved from: http://adsabs.harvard.edu/full/1978LPSC....9.3843G

Gentner, W. (1966). Auf der Suche nach Kratergläsern, Tektiten und Meteoriten in Afrika. *Naturwissenschaften, 53*(12), 285–289. https://doi.org/10.1007/BF00712210

Glass, B. P. (2003, March 17–21). *Australasian microtektites in the South China Sea: Implications regarding the location and size of the source crater* [Abstract #1092]. Abstract submitted to the 34th Lunar and Planetary Science Conference, League City, Texas, United States of America. Retrieved from: https://www.lpi.usra.edu/meetings/lpsc2003/pdf/1092.pdf

Glass, B. P., & Barlow, R. A. (1979). Mineral inclusions in Muong Nong-type indochinites: Implications concerning parent material and process of formation. *Meteoritics, 14*(1), 55–67. https://doi.org/10.1111/j.1945-5100.1979.tb00479.x

Glass, B. P., Huber, H., & Koeberl, C. (2004). Geochemistry of Cenozoic microtektites and clinopyroxene-bearing spherules. *Geochimica et Cosmochimica Acta, 68*(19), 3971–4006. https://doi.org/10.1016/j.gca.2004.02.026

Glass, B. P., & Koeberl, C. (2006). Australasian microtektites and associated impact ejecta in the South China Sea and the Middle Pleistocene supereruption of Toba. *Meteoritics & Planetary Science, 41*(2), 305–326. https://doi.org/10.1111/j.1945-5100.2006.tb00211.x

Glass, B. P., & Pizzuto, J. E. (1994). Geographic variation in Australasian microtektite concentrations: Implications concerning the location and size of the source crater. *Journal of Geophysical Research, 99*(E9), 19075-19081. https://doi.org/10.1029/94JE01866

Glass, B. P., & Simonson, B. M. (2013). *Distal impact ejecta layers: A record of large impacts in sedimentary deposits*. 716 p. Heidelberg; New York: Springer. ISBN 978-3-540-88262-6

Gong, Z. S., & Li, S. T. (2004). *Dynamic research of oil and gas accumulation in northern marginal basins of South China Sea*. 339 p. Science in China Press, Beijing, (in Chinese with English abstract).

Gong, Z. S., Li, S. T., Xie, T. J., Zhang, Q. M., Xu, S. C., Xia, K. Y., … Liu, L. H. (1997). *Continental margin basin analysis and hydrocarbon accumulation of the northern South China Sea*. 510 p. China Sci. Press, Beijing, (in Chinese with English abstract).

Haines, P. W., Howard, K. T., Ali, J. R., Burrett, C. F., & Bunopas, S. (2004). Flood deposits penecontemporaneous with ~0.8 Ma tektite fall in NE Thailand: Impact-induced environmental effects? *Earth and Planetary Science Letters, 225*(1–2), 19–28. https://doi.org/10.1016/j.epsl.2004.05.008

Hartung, J. B., & Koeberl, C. (1994). In search of the Australasian tektite source crater: The Tonle Sap hypothesis. *Meteoritics, 29*(3), 411–416. https://doi.org/10.1111/j.1945-5100.1994.tb00606.x

Hoang, N., Flower, M. F. J., & Carlson, R. W. (1996). Major, trace element, and isotopic compositions of Vietnamese basalts: Interaction of hydrous EM1-rich asthenosphere with thinned Eurasian lithosphere. *Geochimica et Cosmochimica Acta, 60*(22), 4329–4351. https://doi.org/10.1016/S0016-7037(96)00247-5

Hoang, N., Hauzenberger, C., Fukuyama, M., & Konzett, J. (2018, October 16-17). *Cenozoic volcanism in the Bolaven Plateau, southern Laos*. Abstract submitted to the Regional Congress on Geology, Minerals and Energy Resources of Southeast Asia (GEOSEA), Hanoi, Vietnam.

Howard, B. C. (2016). Australia Is Drifting So Fast GPS Can't Keep Up. *National Geographic*. [online]. [Cited 23 September 2016]. Retrieved from: https://www.nationalgeographic.com/news/2016/09/australia-moves-gps-coordinates-adjusted-continental-drift/

Howard, K. T. (2011). Volatile enhanced dispersal of high velocity impact melts and the origin of tektites. *Proceedings of the Geologists' Association, 122*(3), 363–382. https://doi.org/10.1016/j.pgeola.2010.11.006

Howard, K. T., Haines, P. W., Burrett, C. F., Ali, J. R., & Bunopas, S. (2003). Sedimentology of 0.8 Ma log-bearing flood deposits in northeast Thailand and mechanisms for pre-flood deforestation. *Proceedings, 8th International Congress on Pacific Neogene Stratigraphy, Chiang Mai, Thailand*, 49–67.

Huber, H. (2009). INAA of Muong-Nong type tektites and adjacent soil samples. *22nd Seminar Activation Analysis and Gamma-Spectroscopy. Program and Book of Abstracts*. 35.

Izokh, E. P., & An, L. D. (1983). Tektites of Vietnam. Tektites delivered by a comet: A hypothesis. *NASA Report No. NAS 1.7720103; NASA-TT-20103*. Transl. into English from *Meteoritika (Moscow), 42*, 158-170.

Javanaphet, C. (1969). *Geological Map of Thailand; Scale 1: 1,000,000 with Explanation*. Department of Mineral Resources, Bangkok, Thailand.

Jiang, T., Xie, X., Chen, H., Wang, Z., and Li, X. (2015) Geochemistry of pore water and associated diagenetic reactions in the diapiric area of Yinggehai Basin, northwestern South China Sea.

Journal of Earth Science, 26(3), 306–316. https://doi.org/10.1007/s12583-015-0526-y

Jonell, T. N., Clift, P. D., Hoang, L. V., Hoang, T., Carter, A., Wittmann, H., … Rittenour, T. (2017). Controls on erosion patterns and sediment transport in a monsoonal, tectonically quiescent drainage, Song Gianh, central Vietnam. *Basin Research, 29*, 659–683. https://doi.org/10.1111/bre.12199

Jourdan, F. (2012). The ^{40}Ar/^{39}Ar dating technique applied to planetary sciences and terrestrial impacts. *Australian Journal of Earth Sciences, 59*(2), 199–224. https://doi.org/10.1080/08120099.2012.644404

Jourdan, F., Moynier, F., Koeberl, C., & Eroglu, S. (2011). ^{40}Ar/^{39}Ar age of the Lonar crater and consequence for the geochronology of planetary impacts. *Geology, 39*(7), 671–674. https://doi.org/10.1130/G31888.1

Jourdan, F., Nomade, S., Wingate, M. T. D., Eroglu, E., & Deino, A. (2019). Ultraprecise age and formation temperature of the Australasian tektites constrained by ^{40}Ar/^{39}Ar analyses. *Meteoritics & Planetary Science, 54*(10), 2573–2591. https://doi.org/10.1111/maps.13305

Kenkmann, T., Collins, G. S., Wittmann, A., Wünnemann, K., Reimold, W. U., & Melosh, H. J. (2009). A model for the formation of the Chesapeake Bay impact crater as revealed by drilling and numerical simulation. *Geological Society of America Special Papers, 458*, 571–585. https://doi.org/10.1130/2009.2458(25)

Koeberl, C. (1986). Muong Nong type tektites from the moldavite and North American strewn fields? *Journal of Geophysical Research: Solid Earth, 91*(B13), E253–E258. https://doi.org/10.1029/JB091iB13p0E253

Koeberl, C. (1992). Geochemistry and origin of Muong Nong-type tektites. *Geochimica et Cosmochimica Acta, 56*(3), 1033–1064. https://doi.org/10.1016/0016-7037(92)90046-L

Koeberl, C. (1994). Tektite origin by hypervelocity asteroidal or cometary impact: Target rocks, source craters, and mechanisms. *Geological Society of America Special Papers, 293*, 133–152. https://doi.org/10.1130/SPE293-p133

Koeberl, C., Bottomley, R., Glass, B. P., & Storzer, D. (1997). Geochemistry and age of Ivory Coast tektites and microtektites. *Geochimica et Cosmochimica Acta, 61*(8), 1745–1772. https://doi.org/10.1016/S0016-7037(97)00026-4

Koeberl, C., Kluger, F., & Kiesl, W. (1985). Rare earth elemental patterns in some impact glasses and tektites and potential parent materials. *Chemie Der Erde, 44*(2), 107–121.

Koeberl, C., Nishiizumi, K., Caffee, M. W., & Glass, B. P. (2015, July 27–31). *Beryllium-10 in Individual Australasian Microtektites and Origin of Tektites* [Abstract #5187]. Abstract submitted to the 78th Annual Meeting of the Meteoritical

Society, Berkeley, California, United States of America. Retrieved from: https://www.hou.usra.edu/meetings/metsoc2015/pdf/5187.pdf

Korschinek, G., Bergmaier, A., Faestermann, T., Gerstmann, U. C., Knie, K., Rugel, G., … Gostomski, C. L. von. (2010). A new value for the half-life of [10]Be by heavy-ion elastic recoil detection and liquid scintillation counting. *Nuclear Instruments and Methods in Physics Research Section B: Beam Interactions with Materials and Atoms, 268*(2), 187–191. https://doi.org/10.1016/j.nimb.2009.09.020

Lei, C., Ren, J., Clift, P. D., Wang, Z., Li, X., & Tong, C. (2011). The structure and formation of diapirs in the Yinggehai–Song Hong Basin, South China Sea. *Marine and Petroleum Geology, 28*(5), 980–991. https://doi.org/10.1016/j.marpetgeo.2011.01.001

Lei, C., Ren, J., Sternai, P., Fox, M., Willett, S., Xie, X., … Wang, Z. (2015). Structure and sediment budget of Yinggehai–Song Hong basin, South China Sea: Implications for Cenozoic tectonics and river basin reorganization in Southeast Asia. *Tectonophysics, 655*, 177–190. https://doi.org/10.1016/j.tecto.2015.05.024

Liu, Z., Colin, C., Huang, W., Le, K. P., Tong, S., Chen, Z., & Trentesaux, A. (2007). Climatic and tectonic controls on weathering in south China and Indochina Peninsula: Clay mineralogical and geochemical investigations from the Pearl, Red, and Mekong drainage basins: controls on weatherings in S. China. *Geochemistry, Geophysics, Geosystems, 8*(5). https://doi.org/10.1029/2006GC001490

Liu, Z., Zhao, Y., Colin, C., Stattegger, K., Wiesner, M. G., Huh, C. A., … Li, Y. (2016). Source-to-sink transport processes of fluvial sediments in the South China Sea. *Earth-Science Reviews, 153*, 238–273. https://doi.org/10.1016/j.earscirev.2015.08.005

Lodders, K., & Fegley, B. (1998). *The Planetary Scientist's Companion*. 392 p. Oxford University Press on Demand. ISBN: 9780195116946

Ma, P., Aggrey, K., Tonzola, C., Schnabel, C., de Nicola, P., Herzog, G. F., … Klein, J. (2004). Beryllium-10 in Australasian tektites: Constraints on the location of the source crater. *Geochimica et Cosmochimica Acta, 68*(19), 3883–3896. https://doi.org/10.1016/j.gca.2004.03.026

Mark, D. F., Renne, P. R., Dymock, R. C., Smith, V. C., Simon, J. I., Morgan, L. E., … Pearce, N. J. G. (2017). High-precision [40]Ar/[39]Ar dating of Pleistocene tuffs and temporal anchoring of the Matuyama-Brunhes boundary. *Quaternary Geochronology, 39*, 1–23. https://doi.org/10.1016/j.quageo.2017.01.002

Matsuda, J., Maruoka, T., Pinti, D. L., & Koeberl, C. (1996). Noble gas study of a philippinite with an unusually large bubble. *Meteoritics & Planetary Science, 31*(2), 273–277. https://doi.org/10.1111/j.1945-5100.1996.tb02023.x

McDonough, W. F., & Sun, S. S. (1995). The composition of the Earth. *Chemical Geology, 120*(3–4), 223–253. https://doi.org/10.1016/0009-2541(94)00140-4

McHarg, I. L. (1969). *Design with Nature*. Garden City, N.Y.: Published for the American Museum of Natural History [by] the Natural History Press.

Meisel, T., Langenauer, M., & Krähenbühl, U. (1992). Halogens in tektites and impact glasses. *Meteoritics, 27*(5), 576–579. https://doi.org/10.1111/j.1945-5100.1992.tb01079.x

Métivier, F., Gaudemer, Y., Tapponnier, P., & Klein, M. (1999). Mass accumulation rates in Asia during the Cenozoic. *Geophysical Journal International, 137*(2), 280–318. https://doi.org/10.1046/j.1365-246X.1999.00802.x

Mizote, S., Matsumoto, T., Matsuda, J., & Koeberl, C. (2003). Noble gases in Muong Nong-type tektites and their implications. *Meteoritics & Planetary Science, 38*(5), 747–758. https://doi.org/10.1111/j.1945-5100.2003.tb00039.x

O'Keefe, J. A. (1963). *Tektites*. 228 p. The University of Chicago Press.

Orbit 1.2 Software. (1998-2000). Published by Siltec Ltd. Retrieved (in 2011, no longer available) from: http://physics-animations.com/Physics/English/orbit.htm

Pierazzo, E., & Melosh, H. J. (2000). Melt Production in Oblique Impacts. *Icarus, 145*(1), 252–261. https://doi.org/10.1006/icar.1999.6332

Povenmire, H. (2010, July 26–30). *The First Georgia-Area Tektite Found in South Carolina* [Abstract #5222]. Abstract submitted to the 73rd Annual Meeting of the Meteoritical Society, New York, United States of America. Retrieved from: https://www.lpi.usra.edu/meetings/metsoc2010/pdf/5222.pdf

Povenmire, H., & Strange, R. L. (2006, March 13–17). *The First Tektite from Dooly Crisp Counties, Georgia* [Abstract #1002]. Abstract submitted to the 37th Lunar and Planetary Science Conference, League City, Texas, United States of America. Retrieved from: https://www.lpi.usra.edu/meetings/lpsc2006/pdf/1002.pdf

Prasad, M. S., Mahale, V. P., & Kodagali, V. N. (2007). New sites of Australasian microtektites in the central Indian Ocean: Implications for the location and size of source crater. *Journal of Geophysical Research, 112*(E6), E06007. https://doi.org/10.1029/2006JE002857

Rochette, P., Braucher, R., Folco, L., Horng, C. S., Aumaître, G., Bourlès, D. L., & Keddadouche, K. (2018). [10]Be in Australasian microtektites compared to tektites: Size and geographic

controls. *Geology, 46*(9), 803–806. https://doi.org/10.1130/G45038.1

Schmieder, M., & Kring, D. A. (2020). Earth's Impact Events Through Geologic Time: A List of Recommended Ages for Terrestrial Impact Structures and Deposits. *Astrobiology, 20*(1), 91–141. https://doi.org/10.1089/ast.2019.2085

Schmitt, S. R. (2004). Ballistic Trajectory (2-D) Calculator-Computes the maximum height, range, time to impact, and impact velocity of a ballistic projectile. [online]. [Cited 14 November 2020]. Retrieved from: http://www.convertalot.com/ballistic_trajectory_calculator.html

Schnetzler, C. C. (1992). Mechanism of Muong Nong-type tektite formation and speculation on the source of Australasian tektites. *Meteoritics, 27*(2), 154–165. https://doi.org/10.1111/j.1945-5100.1992.tb00743.x

Schnetzler, C. C., & McHone, J. F. (1996). Source of Australasian tektites: Investigating possible impact sites in Laos. *Meteoritics & Planetary Science, 31*(1), 73–76. https://doi.org/10.1111/j.1945-5100.1996.tb02055.x

Schnetzler, C. C., & Pinson Jr, W. H. (1963). The chemical composition of tektites. In: O'Keefe, J. A. (1963) *Tektites* (p. 95–129). The University of Chicago Press.

Schultz, P. H. (1992). Atmospheric effects on ejecta emplacement and crater formation on Venus from Magellan. *Journal of Geophysical Research: Planets, 97*(E10), 16183–16248. https://doi.org/10.1029/92JE01508

Schultz, P. H., Anderson, J. B. L., & Hermalyn, B. (2009, March 23–27). *Origin and Significance of Uprange Ray Patterns* [Abstract #2496]. Abstract submitted to the 40th Lunar and Planetary Science Conference, The Woodlands, Texas, United States of America. Retrieved from: https://www.lpi.usra.edu/meetings/lpsc2009/pdf/2496.pdf

Schultz, P. H., Eberhardy, C. A., Ernst, C. M., A'Hearn, M. F., Sunshine, J. M., & Lisse, C. M. (2007). The Deep Impact oblique impact cratering experiment. *Icarus, 191*(2), 84–122. https://doi.org/10.1016/j.icarus.2007.06.031

Shaw, H. F., & Wasserburg, G. J. (1982). Age and provenance of the target materials for tektites and possible impactites as inferred from Sm-Nd and Rb-Sr systematics. *Earth and Planetary Science Letters, 60*(2), 155–177. https://doi.org/10.1016/0012-821X(82)90001-2

Shuvalov, V., & Dypvik, H. (2013). Distribution of ejecta from small impact craters. *Meteoritics & Planetary Science, 48*(6), 1034–1042. https://doi.org/10.1111/maps.12127

Sieh, K., Herrin, J., Jicha, B., Schonwalder Angel, D., Moore, J. D. P., Banerjee, P., … Charusiri, P. (2020). Australasian impact crater buried under the Bolaven volcanic field, Southern Laos. *Proceedings of the National Academy of Sciences, 117*(3), 1346–1353. https://doi.org/10.1073/pnas.1904368116

Stöffler, D., Gault, D. E., Wedekind, J. E., & Polkowski G. (1975). Experimental hypervelocity impact into quartz sand: Distribution and shock metamorphism of ejecta. *Journal of Geophysical Research, 80*(29), 4062-4077. https://doi.org/10.1029/JB080i029p04062

Stöffler, D., Hamann, C., & Metzler, K. (2018). Shock metamorphism of planetary silicate rocks and sediments: Proposal for an updated classification system. *Meteoritics & Planetary Science, 53*(1), 5–49. https://doi.org/10.1111/maps.12912

Tada, T., Carling, P. A., Tada, R., Songtham, W., Chang, Y., & Tajika, E. (2019, December 9-13). *Constraint on the Location of the Australasian Tektite Impact Event based on the Distribution of the Ejecta Deposits across the Eastern Indochina* [Abstract #NH51C-0786; Poster #0786]. American Geophysical Union Fall Meeting, San Francisco, United States of America. Abstract retrieved from: https://ui.adsabs.harvard.edu/abs/2019AGUFMNH51C0786T/abstract

Trnka, M. (2020, March 16–20). *Notes on Contents of 10Be Isotope in Tektites and Microtektites of the Australasian Strewn Field* [Abstract #1149]. Abstract submitted to the 51st Lunar and Planetary Science Conference, The Woodlands, Texas, United States of America. Retrieved from: https://www.hou.usra.edu/meetings/lpsc2020/pdf/1149.pdf

Trnka, M., & Houzar, S. (2002). Moldavites: A review. *Bulletin of the Czech Geological Survey, 77*(4), 283–302. Retrieved from: http://www.geology.cz/bulletin/fulltext/04trnkafinal.pdf

Vickery, A. M. (1993). The theory of jetting: Application to the origin of tektites. *Icarus, 105*(2), 441–453. https://doi.org/10.1006/icar.1993.1140

Vickery, A. M., & Browning, L. (1991, July 21-26). *Water depletion in tektites*. Abstract submitted to the 78th Annual Meeting of the Meteoritical Society, Monterey, California, United States of America. In: *Meteoritics*, 26, 403. Retrieved from: http://adsabs.harvard.edu/full/1991Metic..26Q.403V

Wasson, J. T. (2003). Large Aerial Bursts: An Important Class of Terrestrial Accretionary Events. *Astrobiology, 3*(1), 163–179. https://doi.org/10.1089/153110703321632499

Wasson, J. T. (2017, March 20–24). *A Thermal-Plume Origin of Layered and Splash-Form Tektites and Libyan Desert Glass* [Abstract #2916]. Abstract submitted to the 48th Lunar and Planetary Science Conference, The Woodlands, Texas, United States of America. Retrieved from:

https://www.hou.usra.edu/meetings/lpsc2017/pdf/2916.pdf

Wei, G., Liu, Y., Ma, J., Xie, L., Chen, J., Deng, W., & Tang, S. (2012). Nd, Sr isotopes and elemental geochemistry of surface sediments from the South China Sea: Implications for Provenance Tracing. *Marine Geology, 319–322*, 21–34. https://doi.org/10.1016/j.margeo.2012.05.007

Whymark, A. (2013, March 18–22). *Review of the Australasian tektite source crater location and candidate structure in the Song Hong-Yinggehai basin, Gulf of Tonkin* [Abstract #1077]. Abstract submitted to the 44th Lunar and Planetary Science Conference, The Woodlands, Texas, United States of America. Retrieved from: https://www.lpi.usra.edu/meetings/lpsc2013/pdf/1077.pdf

Whymark, A. (2018, March 19-23). *Further Geophysical Data in the Search for the Australasian Tektite Source Crater Location in the Song Hong-Yinggehai Basin, Gulf of Tonkin* [Abstract #1078]. Abstract submitted to the 49th Lunar and Planetary Science Conference, The Woodlands, Texas, United States of America. Retrieved from: https://www.hou.usra.edu/meetings/lpsc2018/pdf/1078.pdf

Whymark, A. (2020, August 5–7). *Newly Discovered Muong Nong-Type Layered Impact Glass / Tektites from Paracale, Philippines and Implications for Source Crater Location* [Abstract #2006]. Abstract submitted to the 11th Planetary Crater Consortium Meeting, Hawaii (Virtual), United States of America. Retrieved from: https://www.hou.usra.edu/meetings/crater2020/pdf/2006.pdf

Yan, Y., Carter, A., Palk, C., Brichau, S., and Hu, X. (2011). Understanding sedimentation in the Song Hong-Yinggehai Basin, South China Sea: Sedimentation in the Yinggehai Basin. *Geochemistry, Geophysics, Geosystems, 12*(6), https://doi.org/10.1029/2011GC003533

Zähringer, J., & Gentner, W. (1963). Radiogenic and atmospheric argon content of tektites. *Nature, 199*(4893), 583–583. https://doi.org/10.1038/199583a0